THERMAL CONDUCTION THROUGH AN EVACUATED IDEALIZED POWDER OVER THE TEMPERATURE RANGE OF 100° TO 500°K

by Ronald B. Merrill

George C. Marshall Space Flight Center
Huntsville, Ala.

NASA TN D-5063

THERMAL CONDUCTION THROUGH AN EVACUATED

IDEALIZED POWDER OVER THE TEMPERATURE

RANGE OF 100° TO 500°K

By Ronald B. Merrill

George C. Marshall Space Flight Center
Huntsville, Ala.

NATIONAL AERONAUTICS AND SPACE ADMINISTRATION

TABLE OF CONTENTS

LIST OF ILLUSTRATIONS

LIST OF ILLUSTRATIONS (Concluded)

LIST OF TABLES

THERMAL CONDUCTION THROUGH AN EVACUATED IDEALIZED POWDER OVER THE TEMPERATURE RANGE OF 100° TO 500°K

INTRODUCTION

The Problem

There are three modes of heat transfer: solid conduction, convection, and electromagnetic radiation. The electromagnetic mode involves emission, absorption, and scattering of electromagnetic waves, and it is difficult to deal with theoretically. One important case is the radiative thermal conduction through a powder.

Radiative transfer through a powder is important from many standpoints. In theory, it provides a method of studying scattering of radiation from adjacent particles [1,2,3]. In practice, its importance in astrophysics is testified to by its significant role in the theories of heat transport in stars [4,5], on the lunar surface [6], and in the earth's interior [7]. Because of the insulating properties of a powder, these studies are of interest to the engineer [8]. The nature of the radiative thermal conductivity has not been determined experimentally in spite of all the possible uses and actual applications of radiative transfer.

Several reasons exist for paucity of experimental data. The radiative mode is very small when compared to the heat transported by gas conduction and convection in interstitial spaces. Evidence of this was given by some of the first studies of powders [9,10]. Fortunately, the gas mode can be eliminated by studying the powder in a vacuum. The solid conduction mode inside the particles and between the particles through contacts, however, cannot be eliminated. The value is small because of the constriction of the heat transported across the contact area in common to the particles. In fact, at some temperatures, these two modes are of the same order of magnitude.

The major reason why few measurements are performed as a function of temperature can be illustrated by an example. Before this is done, however, a few basic definitions need to be stated. The actual conductivity is defined

as minus the ratio of the heat flux F to the temperature gradient $\Delta T/\Delta \xi$ in the limit where the temperature range ΔT extends to zero over a distance $\Delta \xi$.

$$K = \lim_{\Delta T \to 0} - F\left(\frac{\Delta \xi}{\Delta T}\right)$$

This equation can be considered as descriptive of the microscopic heat flow, and it is used in deriving the heat transport equation. The effective conductivity K_e is the value measured with a steady state method.

$$K_e = -F(\Delta \xi/\Delta T) \tag{1}$$

The two conductivities are equal only when they can be considered as constant over the experimental temperature range. The dependence of K_e on the range of temperatures confines it as a less useful concept than the actual conductivity. Usually, however, the temperature range is small so that $K_e = K$ is a good approximation, but this is generally not true for measurements on evacuated powders.

For a powder, the value for K_e is small, implying that the ratio in equation (1) is small. The heat flux must be greater than a limiting value determined by the experimental detectivity limits or by reason of extraneous heat fluxes along thermocouples, etc. , or owing to not meeting the initial and/or boundary conditions. Reasonable values of F and K_e are 1 $\mu W/cm^2$ and 10 $\mu W/cm^{2\circ}K$, respectively; hence, the value for the gradient is of the order of 100° K per centimeter. Physical restrictions imposed by the boundary conditions mean that $\Delta \xi$ must be greater than or approximately equal to 1 centimeter which implies ΔT equals about 100° K. The temperature where $K = K_e$ lies somewhere in this 100° K temperature range. This example indicates why measurements of the conductivity with respect to temperature for evacuated powders have not been performed satisfactorily.

Historical Background and Theory

The total conductivity caused by all mechanisms can be found by combining each possible mode in a special way. The rule for combining the modes is analogous to solving for the electrical conductivity from a set of conductivities that is in series and in parallel. For completeness this rule may be stated simply as: (1) for the conductivities in parallel, the resulting conductivity is equal to a simple sum of the component conductivities; and (2) for conductivities in series, the inverse of the resulting conductivity is equal to a simple sum of the inverse of the components. These rules allow each mode to be considered separately.

Of the three possible modes, the gaseous conduction mode at standard pressures and temperatures is by far the predominant one. No wonder gaseous conduction was the prime consideration in the study of powders by the early theoretician. Of course, other modes were considered but only in a way to show that they are negligibly small by comparison.

Lord Rayleigh (1892) was the first to derive an expression for the conductivity of a powder [11]. His model consisted of a cubic array of spherical particles. This special model was later generalized by Burgers [12] in 1919 to include ellipsoidal particles and Russell (1935) who calculated the conductivity of a random distribution of cubes in a cubical array where the faces of any two cubes remain parallel [13]. Experimental evidence by Aberdeen and Laby [9], Kannuluik et al. [10], and recently Wechsler et al. [14] have established the dependence of powder conductivity with respect to gas pressure. At pressures of about 10^{-4} torr and lower, the conductivity is independent of gas pressure and the radiative mode predominates.

Every derivation in the literature of the radiative component of conduction in a powder of which the author is aware supposes explicitly or implicitly two basic assumptions. The first assumption is that a particle in a powder has a uniform temperature when compared to the possible temperature differences between particles. This assumption is a reasonable one because the solid conductivity between points in the same particle is very much larger than the measured conductivities across a contact as between two particles.

The other assumption presumes the particles are completely opaque to thermal radiation. For large particles, this assumption seems reasonable because of the large extinction coefficient for most materials and glasses in

the thermal infrared. By reducing the size of the particles, one could imagine reaching a point where the particles are not completely opaque. One way to distinguish whether or not the particles are opaque is to test to see if the conductivity is a function of particle size. This statement will become obvious later.

Two different approaches are considered. In the following, the particles are considered as opaque. The question of nonopaque particles is treated later.

The derivation of the conductivity arising from electromagnetic radiation can be formalized in a very general manner when the above two assumptions are true. The radiant exchange between two objects (labeled (1) and (2)) can be expressed as

$$R = \sigma F_g (\epsilon_1 T_1^4 - \epsilon_2 T_2^4)$$

where R is the energy exchanged per second and per unit of cross-sectional area perpendicular to the direction of the heat flow, σ is Stefan-Boltzmann's constant, ϵ_1 and ϵ_2 are the emittance factors for object (1) and (2), F_g is the geometric factor, and T_1 and T_2 are the temperatures of objects (1) and (2), respectively. The only case considered here is where the emittance of both objects is the same.

The temperature difference between any two adjacent particles in a powder is small. The radiant energy can now be written as

$$R = 4 \sigma F_g \epsilon T^3 \Delta x \left(\frac{\Delta T}{\Delta x}\right) = K_{rad} \left(\frac{\Delta T}{\Delta x}\right)$$

where $\Delta T = T_1 - T_2$. T lies somewhere in the interval between T_2 and $T_2 + \Delta T$, Δx is some characteristic effective separation distance between the two objects, and K_{rad} is the conductivity which is caused solely by radiation. Solving for the value of K_{rad},

$$K_{rad} = 4 \sigma \epsilon F_g \Delta x T^3$$

4

The problem now is expressing K_{rad} in terms of measurable quantities which in turn means deriving expressions for the geometric factor (F_g) and the path length of the radiation Δx by considering specific models.

Wesselinck (1960) proposed as a model the powder be considered as stratified into layered slabs with radiative transfer occurring between slabs [15]. His expression for the radiative conductivity is given by

$$K_{rad} = \frac{4 \, \epsilon \, \sigma \, d}{(2 - \epsilon)} \, \frac{1}{(1 - p)} \, T^3 \tag{2}$$

where d is the diameter of the particles, p is the porosity, and (1 - p) is the percent of the volume filled by the particles.

Laubitz (1959) modified Russell's derivation slightly and obtained the following radiative term [16].

$$K_{rad} = \frac{4 \, \sigma \, \epsilon \, d}{(1 - p)} \, T^3 \, [1 - (1 - p)^{2/3} + (1 - p)^{4/3}] \tag{3}$$

Schotte (1960) obtained an expression by considering a combination of a radiative mechanism between the surfaces, along with radiation in series, with the conduction through the spherical particles [17].

$$K_{rad} = \frac{(1 - p)}{\dfrac{1}{K_s} + \dfrac{1}{K_{ro}}} + p \, K_{ro} \tag{4}$$

$$K_{ro} = 4 \, \sigma \, \epsilon \, d \, T^3$$

This equation can be simplified by noticing that the intrinsic solid conductivity K_s (at least for those cases that are of interest in this paper) is much greater than the radiative term K_{rad} so that

$$K_{rad} \doteq 4 \, \sigma \, \epsilon \, d \, T^3 \, . \tag{5}$$

5

Notice that equations (2), (3), and (5) have one property in common: they predict K_{rad} to be proportional to T^3. Except for equation (5), K_{rad} monotonically increases with the porosity.

Foregoing arguments have been restricted to the cases where a particle is considered as opaque. At this time, the case of the transparent particle is treated. Consider the well-known formula for the thermal conductivity of a gas [18]:

$$K = \frac{1}{3} C \, v \, \Lambda$$

where C is the heat capacity of the gas per unit volume, v is the average velocity of the gas particles, and Λ is the mean free path. In analogy, the photons in a system are considered as a photon gas, the restrictive being that boundaries are far enough away not to affect the properties of the gas. The heat capacity of this photon gas is the partial derivative of the energy density. The energy density is given by the expression

$$U = \frac{4}{c} \sigma \, T^4$$

where c is the velocity of light. The expression for the conductivity becomes

$$K_{rad} = \frac{16}{3} \sigma \, T^3 \, \Lambda \quad . \tag{6}$$

The mean free path (Λ) may depend on the temperature. The mean free path can be represented by the equation

$$\Lambda(T) = \int_0^\infty x \, f(x, T) \, dx$$

where $f(x, T)$ is the distribution function of the distance traveled by a photon or

$$f(x, T) = \int_0^\infty \frac{U(\lambda, T)}{U(T)} f'(x,\lambda) \, d\lambda$$

where $U(\lambda, T)$ represents the energy density of the photons with a wavelength between λ and $\lambda + d\lambda$, $U(T)$ is the total energy density of the photons, and $f'(x,\lambda)$ is the distribution function of the distance traveled by a photon along the direction of the gradient with a wavelength between λ and $\lambda + d\lambda$. The distribution function for a simple case is equivalent to Lambert's absorption law so that

$$f'(x,\lambda) = \exp(-\alpha(\lambda) x) / \int_0^\infty \exp(-\alpha(\lambda) x) \, dx$$

where $\alpha(\lambda)$ is the absorption coefficient. If the absorption coefficient is independent of the wavelength where $U(\lambda, T)$ has significant values, $f(x, T)$ is independent of temperature, and, consequently, the mean free path would be also. Of course α is not in general independent of wavelength, but various arguments can be made to point out that the change in Λ caused by a temperature change is small compared to T^3 over the same range. These arguments are tenuous; one reason is that little information is available concerning the magnitude of the absorption coefficient or related constants as a function of wavelength.

The approach followed in this report assumes that the predominant temperature dependence in the radiant conductivity is the temperature cubed dependence. The data will be analyzed with this assumption in mind, and this assumption will also be tested.

So far gaseous and radiative conduction have been discussed. One last mode remains — that of solid conduction. For solid conduction, heat is transferred in series through a particle and then across the contact between the particles.

The contact resistance would logically appear to be much greater than through the solid because of the restricted area of the contact. Measurements indicate that it is indeed several orders of magnitude greater [19]. This means that the effective solid conduction is equal to essentially the contact conduction.

A simple model of contact conduction between spherical particles has been developed by Halajian et al.[20] so that

$$K_{sol} = (1 - p) \left(\frac{\pi \rho g (1 - \nu^2)}{E} \right) K_s z^{1/3} \tag{7}$$

where ρ is the density of the powder, g is the acceleration caused by gravity, ν is Poisson's ratio, E is the modulus of elasticity, K_s is the intrinsic thermal conductivity of the material, and z is the depth of the powder. The dependence of K_{sol} on depth z is a result of considering a force between two particles as due only to the weight of the particles above it. The contact conduction may now be added to the other modes of conduction.

All major modes of heat transfer in a powder have been considered. The expressions developed for each mode can be added as described previously. The major restriction of the heat flow is between the particles of the powder. Heat flows in parallel between the particles by radiative transfer and across the contacts as discussed above.

Adding the solid term to the radiative term in equations (2), (3), and (5), respectively, results in the following expressions of

$$K = (1 - p) \left(\frac{\pi \rho g (1 - \nu^2)}{E} \right) K_s z^{1/3} + \frac{4 \epsilon \sigma d}{(2 - \epsilon)} \frac{1}{(1 - p)} T^3, \tag{8}$$

$$K = (1 - p) \left(\frac{\pi \rho g (1 - \nu^2)}{E} \right) K_s z^{1/3} + \frac{4 \epsilon \sigma d}{(1 - p)} T^3 [1 - (1 - p)^{2/3} + \ldots], \tag{9}$$

and

$$K = (1 - p) \left(\frac{\pi \rho g (1 - \nu^2)}{E} \right) K_s z^{1/3} + (4 \epsilon \sigma d) T^3 . \tag{10}$$

A few values of K have been measured by others usually with a large temperature differential. Watson attempted to overcome this problem by assuming K to be of the form $K = AT^3 + B$ [21]. Notice that this equation is nearly the same, with respect to temperature, as equations (8), (9), and (10) because the intrinsic thermal conductivity of an insulator is nearly constant. The values of A and B were found from three measurements covering

different temperature ranges for several types of powders including glass microbeads. His apparatus consisted chiefly of a platter containing the powder in a vacuum chamber. The chamber walls were cooled to liquid nitrogen temperatures. Heat was supplied to the bottom of the platter, and the temperature and the heat flux at the surface were measured with a radiometer. This method belongs to the class of steady state methods. About 24 hours were required before equilibrium could be approached.

Bernett et al. have developed a transient method and have made several conductivity and diffusivity measurements of olivine basalt and silica sand [22,23]. This method consisted of a cylindrical sample surrounded by a heat reservoir. Thermocouples with leads parallel to the axis were spaced on a diameter. After equilibrium had been established a step function was applied on the heat reservoir by introducing liquid nitrogen. The conductivity and diffusivity values were found from the curve of the temperature recorded by the axial thermocouple with respect to the time. One measurement takes slightly less than 24 hours after initiation. For the case of powders in a vacuum, temperature differentials during the test were on the order of 100° K. An average temperature was assigned to the measured conductivity. Plots of the conductivity were independent of temperature.

A research group at Arthur D. Little Co. has published a large number of papers concerning measurements of powders [14]. This group has measured powders with a probe method, a line heater source (LHS) method, and a guarded cold plate method.

The cold plate method is a steady state method consisting of placing a sample between two plates [24]. One plate is heated, and the other is in contact with a liquid at its boiling point and acts as a heat reservoir. Heat is applied, and the rate of boil-off of the heat reservoir fluid is a measure of the heat flux. The temperatures of the plates are known so that the conductivity is found from a simple calculation using the steady state equation. This method is called a guarded plate method when the plates are concentrically divided such that only the values of the middle plate are used in the calculation. Temperature gradients between the two plates were of the order of 100° K. The method is restricted to heat reservoir fluids that boil off readily and have a well-defined boiling point in the temperature range of interest. Obtaining an adequate vacuum required long outgassing times.

The probe method consists of a long tube containing a heater and a thermometer [25]. The tube is constructed of a good conductor when compared to the material being measured arguing that the temperature is relatively

uniform across the probe. An asymptotic solution for the cylindrical heat transport equation with boundaries at infinity is proportional to the $\log_e$ of the time. The conductivity is calculated from the proportionality constant. One problem arises in using the asymptotic solution because equilibrium is difficult to establish and/or because of the source of heat fluxes from the outside boundary. The exact solution, near the asymptotic region, can be employed by using a graphical curve fitting method [26]. This improvement also means that one measurement can be taken after equilibrium has been established in about 1 hour's time instead of several hours by the older method. Establishing equilibrium requires about 24 hours. Unfortunately, a significant amount of heat is lost along the probe when the conductivity is low as in the case of powders [27]. This problem is not as serious in the line heater source (LHS) method.

The geometry of the LHS method consists essentially of two long parallel wires [28]. One wire is used as a heater, and the other is a thermocouple. The solution of the heat transfer equation is of the same form as the probe method solution although differently interpreted. In the probe method the temperature of the heater is monitored while the powder is monitored for the LHS method. The same graphical method is used to reduce the data.

The data of Arthur D. Little are insufficient to indicate if the conductivity is dependent upon temperature or to verify or distinguish between equations (8), (9), and (10) [14]. Recently some data from the LHS method became available showing that there is a temperature dependence [29].

Proposed Research

The theoretically derived equations (8), (9), and (10) state that the conductivity should definitely be temperature dependent. Watson assumed this fact and measured the effect of changing the porosity and particle size for spherical microbeads, pumice powders, and several other materials. But Bernett et al. measured the effect of changing the porosity and particle size temperature dependence. Obviously, one goal would be to measure the conductivity as a function of temperature, but this is a very difficult thing to do. One reason is that the temperature range should not be so large as to obscure the proper temperature that should be assigned to the measured conductivity.

10

The goals that were decided upon as a subject for this research were:

(1) to find a method suitable for measuring the thermal conductivity as a function of temperature,

(2) to measure the conductivity as a function of temperature of an idealized powder that conforms to the assumptions made in developing the theoretical expressions, and

(3) to compare these measurements with those that have already been made and with the theoretical expressions.

METHOD OF MEASUREMENT

Analysis of Several Methods

In this analysis only a few methods are considered in detail. Many methods are obviously not suitable for measuring low thermal conductivities. Only methods which have been used in the past or which are especially attractive are considered. The method finally chosen is called the Differential Line Heat Source method and is abbreviated as DLHS.

Steady State Methods. The class of steady state methods was eliminated from consideration because the temperature dispersion of nonsteady state methods is smaller. This fact is obvious when steady state methods are pictured as a limiting condition of the transient case where the change in the heat flow approaches zero. More than this, however, there exist special geometries that have not been duplicated by steady state methods. In these, the heat source and temperature sensor are close together. Only the rate of change in the temperature is needed, and not the gradient, so no errors are introduced because of their nearness.

Probe Methods. The probe method beongs to that class in which the temperature is monitored at the source of the heat flux. Measurements taken by this method usually have been restricted to the better conductors because of the size of the heat loss through the length and out of the probe. Experience with probes constructed of fine needles indicates that they still have axial flow of a significant proportion.

A new probe method — called a platinum wire probe — has been devised and tested. It has the advantages associated with all probe methods of being very sensitive so that the conductivity of evacuated powders can be measured with a very small temperature change (~3° K). The axial heat flow is minimized in the construction by a platinum wire 0.001 inch in diameter and about 15 centimeters in length.

The axial heat which does occur is subtracted by a balance bridge method. Actually, two platinum wires of unequal length are placed in the material to be measured. Each wire is connected on the opposite arms and equal resistances in the other arms of the bridge. The bridge has the property of cancelling the axial heat flow of the longer wire by the shorter one. Preliminary measurements demonstrated the utility of this method, but it is very sensitive to how well the sample reaches equilibrium. When the change is in the order of about 3° K, a change of about 0.1° K will be noted in the asymptote region. The method requires that a temperature difference, and a corresponding time difference, be taken in the asymptotic region. The initial conditions reduce to the requirement that the initial temperature must be stable within about 0.001° K over the asymptotic period of the measurement (~60 sec). This restriction is very difficult to satisfy. Increasing the power applied increases the total temperature change and somewhat relaxes the restrictions imposed by the initial conditions (IC), but the power increase is accompanied by other problems. Jagged curves are sometimes obtained; these can be reproduced by shaking the container. The platinum wire apparently meanders through the powder while being heated. In the meantime, another highly promising method was suggested by work that had been done previously with a pulse method.

Pulse Method. A pulse method has been developed using a cylindrical geometry. The physical configuration is essentially the same as the LHS method; however, the heater is pulsed with a short burst of energy. A test on a powder can be completed in a few minutes. The conductivity can be measured, depending upon how much energy is released with the short burst of current through the heater wire. The theory is simple for a short burst but becomes rather complicated when the burst is longer than about one-tenth of the time that it takes the temperature to reach its maximum. Very short bursts mean that the heater wire becomes very hot as does the material around it.

The same form of the solution may be obtained by differentiating the integral with respect to time, the difference being that now a steady rate of power is supplied to the heater instead of a pulse, and the time rate of change of the temperature is measured instead of the temperature. This new method is called the DLHS method.

Theory of Measurements

The theory of all these methods was developed by using a Green's-function approach. The derivation applies to a cylindrical geometry where there are no heat fluxes in the direction of the axis of the heater. Figure 1 depicts the geometry considered and defines some of the terms used. For the following derivation the conductivity is assumed to be constant. This assumption will be tested later to see how much error is introduced.

The heat transfer equation is given by

$$K \nabla^2 T = \rho C (\partial T/\partial t) \qquad (11)$$

where ρC is the heat capacity per unit volume, and K is the conductivity. Consider the change of coordinates: $T = v + T_0$ where T_0 is the initial temperature at a point "a."

The heat transfer equation now becomes

$$k \nabla^2 v = \partial v/\partial t$$

where $v = T - T_0$, and k is the thermal diffusivity. The solution may be written in terms of a Green's function and is given by [30]

$$v(\vec{r}, t) = \iint G(\vec{r}, \vec{r'}, t) \, v(\vec{r'}, t' = 0) \, dx' \, dy'$$

2b = DIAMETER OF HEATER WIRE

OUTER CONTOUR

HEATER WIRE (RADIUS = b = .0005")

THERMOCOUPLE LEADS (RADIUS = .0005")

CIRCULATING LIQUID HOLES

CU BLOCK

a ≈ .5mm

FIGURE 1. PLANAR GEOMETRY CONSIDERED IN THEORY OF MEASUREMENT

$$+ k \int_0^t \left[\int \text{contour} \left\{ G(\vec{r},\vec{r}';t-t') \left(\frac{\partial v(\vec{r}',t')}{\partial N} \right) \right\} dl' \right] dt'$$

$$- k \int_0^t \left[\int \text{contour} \left\{ v(\vec{r}',t') \left(\frac{\partial G(\vec{r},\vec{r}';t-t')}{\partial N} \right) \right\} dl' \right] dt'$$

(12)

where $\partial/\partial N$ is the normal partial derivative drawn outward from the region of interest, $G(\vec{r},\vec{r}'; t-t')$ is the Green's function which satisfies the boundary conditions and is defined more fully below, and $v(\vec{r}', t' = 0)$ is the initial temperature difference distribution over the two-dimensional plane of interest. The points in space denoted by the variables $\vec{r}$ and $\vec{r}'$ are called the field points and source points, respectively. The meaning of these terms becomes clear when Green's function is defined.

The Green's function has the following mathematical properties:

1. $G = G(\vec{r},\vec{r}'; t-t')$ for all $t > t'$

2. $k \nabla^2 G = \partial G/\partial t$

3. $k \nabla'^2 G = -\partial G/\partial t'$

4. $\int_{\text{all space}} G(\vec{r},\vec{r}'; 0)\, dx'\, dy' = 1$

   and $G(\vec{r},\vec{r}'; 0) = 0$ iff $\vec{r} \neq \vec{r}'$.

Physically, the Green's function is the solution of the heat transfer equation for a point source at time $t = t'$. The source is located at $\vec{r}'$, and this point is called the source point. The Green's function at the field point $\vec{r}$ is the temperature at that point for a unit heat source located at $\vec{r}'$.

14

The first term in equation (12) represents the effect of the initial temperature not being equal to T_0 everywhere. For this discussion, suppose that it does. The case where the first term is different from zero will be considered later.

The second term in equation (12) represents the portion of the solution that is credited to the heat fluxes introduced by sources on the boundary. As will be seen, this term is the largest for the cases considered here.

The third term in equation (12) represents the effect of having a finite boundary or, in other words, a finite heater wire.

An expression for Green's function can be found from an application of a Fourier transformation to the definition with the boundary at infinity [31].

$$G(r, r'; t - t') = \frac{1}{4\pi k(t - t')} \exp\left(\frac{(\vec{r} - \vec{r'})^2}{4k(t - t')}\right). \tag{13}$$

This expression is substituted into the solution as formulated in equation (12), and the contour integral is integrated so that

$$v(a, t) \doteq k \int_0^t \left(-\frac{dv}{dr}\right)_b G_a \, 2\pi b \, dt'$$

$$- k \int_0^t v_b \, G_a \left(\frac{2a}{4k(t - t')}\right) 2\pi b \, dt'. \tag{14}$$

The field point was considered at a and the source points were considered at b where a>>b.

Equation (14) can be simplified by letting $x = a^2/4kt$ and $x' = a^2/4k(t - t')$. Notice also that the rate of heat per unit length of the heater is given by

$$F = -2\pi b K \, (\partial v/\partial r)_b.$$

With these simplifications in mind, the solution becomes

$$v(a,t) = \left(\frac{F}{4\pi K}\right) \int_X^\infty \left(\frac{1}{x'}\right) \exp(-x') \, dx'$$

$$- \int_X^\infty v(b,t) \left(\frac{b}{a}\right) \exp(-x') \, dx' \; .$$

The second term in this equation can be shown to be small compared to the first for the case where a>>b. Rather than interrupt the derivation to prove the relative size, this will be done for the particular method and geometry that is finally selected in Appendix A. The solution may now be written as

$$v(a,t) = \left(\frac{F}{4\pi K}\right) \int_X^\infty \frac{1}{x'} \exp(-x') \, dx' \; . \tag{15}$$

Relationship of Theory of Measuring to Methods

<u>Probe and Line Heater Source Methods</u>. The heat flux F is constant for the probe and line heater source methods. The solution may be identified with the exponential function [32] where

$$v = (F/4\pi K) \int_X^\infty (1/x') \exp(-x') \, dx' = -(F/4\pi k) \, Ei(-a^2/4kt), \tag{16}$$

For the case of x being small

$$v = (F/4\pi K)(\log(1/x) - \gamma + x - x^2/4 + \dots) \tag{17}$$

and $\gamma = 0.5772157$.

The value for the conductivity can be determined by curve fitting with equation (16) or where x << 1 from the slope of the data plotted on log paper.

$$K = \left(\frac{F}{4\pi\Delta v} \right) \log(t_1/t_2) \qquad (18)$$

where $\Delta v = v_2 - v_1$ and the time the temperature changes from the original temperature at point a is t_1, etc. Notice that only a change in temperature and the heat flux need be determined.

Pulse Method. The pulse method differs from the above only through the heat flux F where F vanishes for some time t greater than a given time τ. For this case where $t \gg \tau$, the solution follows from equation (15) with

$$v = (1/K) \int_0^\tau (F/4\pi(t - t')) \exp[-a^2/4k(t - t')] \, dt'$$

$$\doteq (1/4\pi Kt) \exp[-a^2/4kt] \int_0^\tau F \, dt' \qquad (19)$$

or

$$v \doteq (Q/4\pi Kt) \exp[-a^2/4kt] \; . \qquad (20)$$

The quantity Q is the total heat input in the pulse per unit length of the heater wire.

Differentiated Line Heater Source Method. The DLHS method was the method selected and used in measuring the thermal conductivity as reported herein in the section MEASUREMENTS.

The DLHS method differs from the LHS method only in that the LHS temperature is differentiated with respect to time. From equation (16)

$$\left(\frac{dv}{dt} \right) = \left(\frac{dv}{dx} \right) \left(\frac{dx}{dt} \right) = \left(\frac{F}{4\pi K} \right) \left(\frac{1}{x} \right) \exp(-x) \, (a^2/4kt^2) \qquad (21)$$

or

$$\left(\frac{dv}{dt} \right) = \frac{F}{4\pi Kt} \exp(-a^2/4kt) \; . \qquad (22)$$

The solution is in the form of a pulse, as expected, where the front part behaves as $\exp[-a^2/4kt]$ and the back part as $1/t$. Several ways of finding the diffusivity and conductivity exist depending on which characterization is convenient.

Using the maximum value for (dv/dt) and the corresponding time t_m, the conductivity is written below as

$$K = F/4\pi e \, (dv/dt)_m \, t_m \, . \tag{23}$$

From Figure 2, which is a plot of the solution, a more precise characterization is found by considering the time it takes to reach half of the maximum. The constant $t_{1/2}/t_m = 0.37337$ was found by a numerical iteration of equation (20). The conductivity now becomes

$$K = (0.37337) \, F/4\pi e \, (dv/dt)_m \, t_{1/2} \, , \tag{24}$$

Comparison between Methods

All of the methods mentioned in the preceding subsection Theory of Measurements were tried. The difficulties cited for each one were sufficiently large to encourage further search until the last method (DLHS method) was discovered. It has many of the advantages of the former methods but few of their faults.

Theoretically, each method has roughly the same accuracy assuming the initial conditions for the particular solution could be met. The proper IC in reality were quite difficult to obtain. A solution can be found for the DLHS method when the IC are of a more general form than considered previously. Consider the initial temperature to be of any form. The first term in equation (12) is now not equal to zero and can be expressed as a power series. Suppose the temperature is changed at the boundaries by a step function, for example, by surrounding the cylindrical geometry with liquid nitrogen or hot oil, etc. The temperature at a point (after initial transients) is described quite well by the first few terms of a power series. In fact, the change is quite linear for
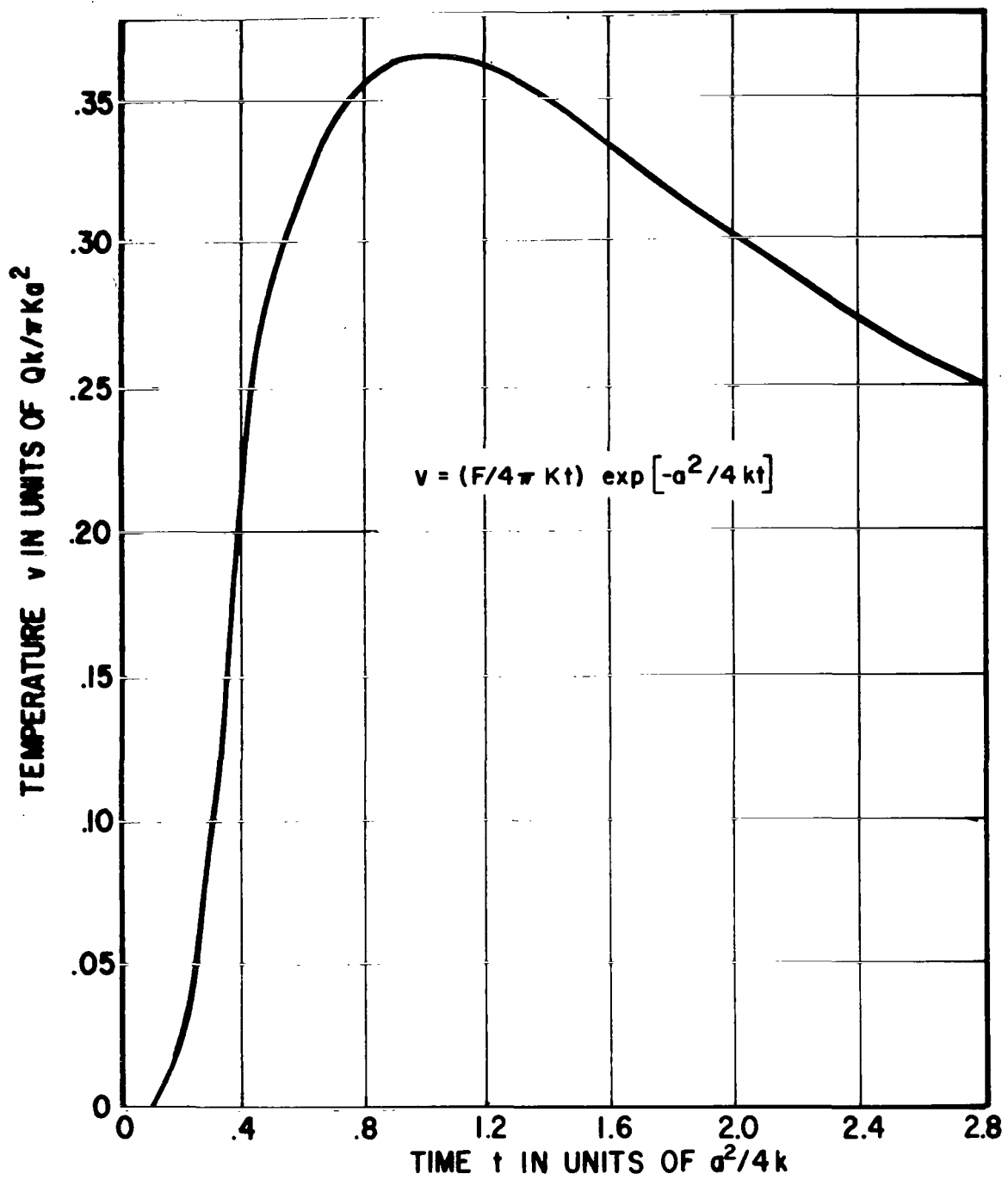
FIGURE 2. PLOT OF SOLUTION FOR DIFFERENTIATED LINE
HEATER SOURCE METHOD

evacuated powders over a period of about an hour. This means that the solution to the heat transfer equation with IC as described above can be written as

$$v = A_0 + A_1 t + \int_0^t \frac{F}{4\pi K (t - t')} \exp[-a^2/4 k (t - t')] \, dt' \tag{25}$$

where A_0 and A_1 are constants.

The DLHS method considers the derivative of the temperature change as in equation (20); hence,

$$\frac{dv}{dt} = A_1 + \frac{F}{4\pi K t} \exp(a^2/4 k t) \tag{26}$$

and

$$K = (0.37337) \ F/4\pi e \left(\frac{dv}{dt} - A_1 \right)_m t_{1/2}. \tag{27}$$

With this arrangement, the conductivity can be measured within a few minutes while the temperature is changing uniformly.

EXPERIMENTS USING DIFFERENTIATED LINE HEATER SOURCE METHOD

Experimental Arrangement

The heater and thermocouple assembly for samples 2 and 3 was constructed as shown in Figure 3. The heater is a 0.001-inch diameter constantan wire. It is attached to copper posts on a glass base. The other parallel wire is an iron constantan thermocouple also 0.001 of an inch in diameter. The thermocouple junction is located midway between two posts. The iron lead is attached to an iron post and the constantan lead to a constantan post. Similar wires are run to the exit electrical connector in the vacuum system. The two wires are usually about 0.06 centimeter apart and about 15 centimeters long.
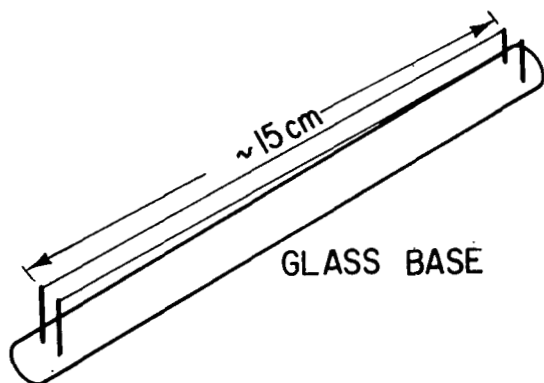
FIGURE 3. HEATER AND THERMO-
COUPLE ASSEMBLY FOR SAMPLES
2 AND 3

Most of the reported measure-
ments were made with a different
experimental arrangement. The
arrangement is changed so that the
temperature range can be increased
from 200° to 400° K to 100° to 500° K.
This is accomplished by constructing
a new line heater and thermocouple
assembly and placing it into a glass
tube which runs outside of the vacuum
system. The new line heater and
thermocouple assembly is shown in
Figure 5. The wires and dimensions
are the same as previously described.
The exception is now that the length
of the wires is of the order of 20
centimeters. The supports are made
of glass and glued together with a
ceramic. The wire heater and ther-

The sample holder was placed,
for the initial runs and for samples 2
and 3, into slots of a massive hollow
stainless steel block. The block is
shown in Figure 4. Two pipes carry
a fluid through the block. The fluid is
either liquid nitrogen, air, or oil. The
block is used as a means of controlling
the initial conditions. It is insulated
from the surroundings by aluminum
foil, and the bottom rests on powder
insulation. The highest temperature
that the samples can reach in this con-
figuration is about 400° K. The cham-
ber is evacuated for several days
while the sample is maintained at this
temperature.
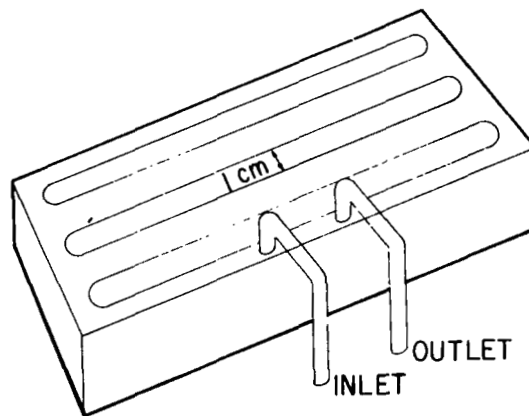
FIGURE 4. SAMPLE HOLDER FOR
SAMPLES 2 AND 3

mocouple assembly is placed into the glass tubes as depicted in Figure 6. They
open into the vacuum chamber through the base plate. The powder is put into
a container inside the vacuum chamber, and the chamber is evacuated. The tube
is brought to a temperature of about 500° K by a nicrome wire heater surrounding
the tube. The powder is slowly poured into the tube from the container while

posts

glass beams

FIGURE 5.   NEW LINE HEATER
AND THERMOCOUPLE ASSEMBLY

still in a vacuum over a period of 8 hours. This procedure ensures that the powder is thoroughly outgassed. Poorly outgassed materials exhibit erratic measured values over a period of time.

The temperature of the tube was controlled by submersing it in LN_2 or by heat supplied from the nicrome heater. The rate of change of the temperature is controlled by the radiation shielding of a dewar, evaporating LN_2, and/or the heater.

The electrical hookup is depicted in Figure 7. The voltage applied across the line heater is supplied by the Fluke precision dc power supply model 301E. Constantan has a low thermal coefficient of resistivity so that the power input remains constant during a measurement. The temperature of the powder is measured at the junction through balancing a Leeds and Northrop K-3 universal potentiometer until a null condition is reached. The reference junction is maintained at the triple point by a Joe Kaye thermocouple reference system. Amplifiers (1) and (2) are Leeds and Northrop dc microvolt amplifiers model 9835. The differentiating circuit differentiates the zero to 1 volt output of amplifier (1). Figure 8 is a schematic of the differentiating circuit with the appropriate values of the components marked. The constant rate of change term was initially bucked to a null condition with potentiometer (2) which is constructed from a battery and a variable resistor. Figure 9 is a typical trace of a run on the strip chart recorder. All the pertinent data that were taken are shown.

A series of runs begins as follows. After the sample is outgassed, the temperature is changed to some initial temperature. The electronics is allowed to warm up and stabilize during this time. The scale factors on amplifiers (1) and (2) are set so that they will not over-run during a test. The rate of change is next subtracted from the output of the differentiation circuit by setting

22
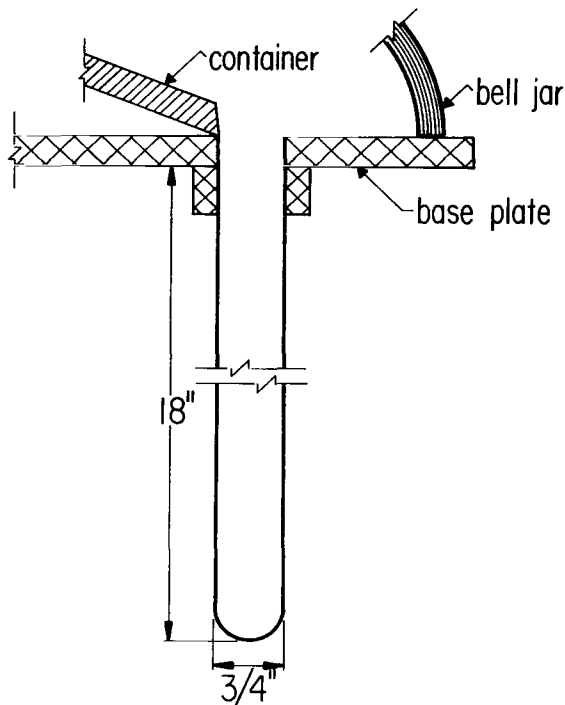
FIGURE 6. GLASS TUBE SAMPLE
HOLDER

potentiometer (2). The temperature is measured by potentiometer (1), and then the run is initiated almost immediately by applying a voltage across the line heater.

Data Reduction

The general form of equation (22) in the section METHOD OF MEASUREMENT is not explicitly in terms of the measured quantities. For example, the heat flux F per unit length of the heater is given in terms of the measured voltage V, current I, and length of the heater wire L so that

$$F = VI/L. \tag{28}$$

Somewhat more difficult is expressing the time rate of change of the temperature dv/dt in terms of measured quantities. The voltage generated by the thermocouple is related to the temperature by a thermoelectric coefficient by the expression

$$e_t = \alpha v \tag{29}$$
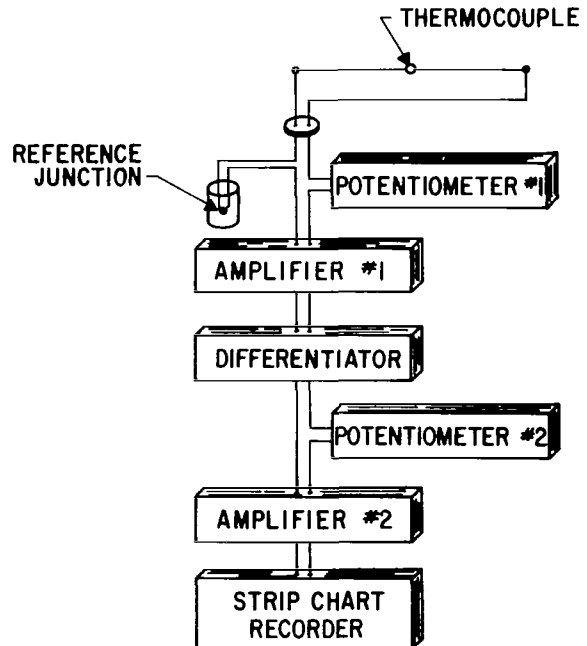
FIGURE 7. DEPICTION OF ELEC-
TRICAL HOOKUP

23
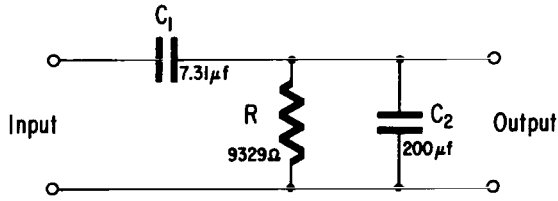
FIGURE 8. SCHEMATIC OF DIFFERENTIATING CIRCUIT

where e_t is the voltage generated by the thermocouple, and α is the thermoelectric coefficient which is a function of temperature. The amplified thermocouple voltage signal signified by e_1 becomes

$$e_1 = e_t/S_1 \qquad (30)$$

and has a value between zero and 1 volt. The quantity $1/S_1$ is the gain factor of amplifier (1).

The voltage e_1 is differentiated by the differentiating circuit resulting in a signal e_d where

$$e_d = (e_c/100)\,S_2 . \qquad (31)$$

and where RC is the time constant of the differentiating circuit. The quantity e_d is the voltage input to the second amplifier and is related to the chart reading of the recorder e_c.

Actually e_c was calibrated in units of centivolts. The value of $(e_c/100)$ is in volts. This relation between e_c and e_d is given by

$$e_d = RC(de_1/dt) .$$

RUN NO. 352
SAMPLE NO. 5
TEMPERATURE 468°K
TIME 12.0 sec
ECM (scale reading) 0.49 volt
S₁   1000
S₂   200
V   1.70 volts
I   12.1 milliamp
L   13.57 cm

$t_{1/2} = 12$ sec

TIME   5 sec   START

FIGURE 9. TYPICAL TRACE OF RUN ON STRIP CHART RECORDER

$$(32)$$

The gain of amplifier (2) is $1/S_2$. Solving for dv/dt from equations (28) through (32) in terms of the measured or known quantities,

$$(dv/dt) = (1/\alpha RC) S_1 S_2 (e_c/100) . \tag{33}$$

The conductivity can now be expressed as

$$K = \frac{VI \alpha RC}{4 \pi L S_1 S_2 (e_c/100) t} \exp(-a^2/4kt) . \tag{34}$$

Three methods can be used to reduce the strip chart data to find the value of the conductivity. These methods are described briefly in the following paragraphs.

Method 1 consisted of using the maximum chart reading and substituting into equation (24) of the METHOD OF MEASUREMENT section. For this case

$$K = 0.37337 B_0 B_1/(\exp(1) e_{cm} t_{1/2})$$

$$B_0 = VI/4 \pi L \tag{35}$$

$$B_1 = (RC \alpha 100)/S_1 S_2 .$$

Method 2 uses a least square adjustment of the conductivity (K) and the parametery $y = a^2/4k$. Equation (34) may be rewritten in the form of

$$e_{ci} = \left(\frac{B}{K t_i}\right) \exp(-y/t_i) . \tag{36}$$

where

$$B = \frac{VI \alpha RC}{4 \pi L S_1 S_2 (1/100)} .$$

The data are in the form of the measured voltage (e_{ci}) versus the time (t_i). The subscript i labels the points picked. The deviation (f) is given by

$$f = \sum_{i=1}^{N} \left[e'_{ci} - \left(\frac{B}{K t_i} \right) \exp(-y/t_i) \right]^2 . \tag{37}$$

The least squares adjustment involves changing the parameters K and y such that the deviation (f) is a minimum. The quantity e_c was the actual chart reading. The minimization was performed by a numerical method called "A Variable Metric Minimization Scheme" [33]. This process requires the initial guesses of K and y and also an estimate of how accurately they are known. The program, as obtained from Dr. D. L. Decker, was modified and put in a general subprogram format. Fortran IV was the language used. The computations were performed on IBM 7040 and 7094 computers.

The third and last method of evaluating the conductivity is similar to the first. Remember the output of the strip chart is in the form of a pulse. Two places occur where the pulse is equal to one-half of the maximum. The first method uses the first point where the voltage increases to one-half of its maximum value. The voltage decreases after the maximum has been reached and asymptotically approaches the initial voltage. The third method uses the point where the voltage decreases to one-half of its maximum value where

$$t'_{1/2} = 4.316 \, t_m \tag{38}$$

Equation (35) then becomes

$$K = 4.316 \, B_0 \, B_1 / (\exp(1) \, e_{cm} \, t'_{1/2}) \tag{39}$$

where equation (39) is the governing equation used by this method.

26

Sources of Errors

The greatest source of systematic errors for the particular experimental arrangement used in this study was calibration. The predominant one was the uncertainty of the value of RC. The absolute value of C was determined within plus or minus 10 percent. The voltage V, current I, and length of the heater wire L and all other sources of calibration error were negligibly small in comparison. Of particular interest is the way in which the length of the heater wire was found. The resistance of a known length of wire was measured. The resistance of the wire on the assembled sample holder was also measured. A simple proportion gives the length accurate to about 0.3 percent or less.

A conservative estimate of how well the chart could be read was plus or minus 0.01 volt. The precision with which time could be read depended upon the chart speed used, but usually it was about 1 second. The degree of this error rests upon the selected method of data reduction. The uncertainty in the conductivity using method 1 was within one to ten percent depending on the particular measurement and data trace. For method 2 and method 3 a reasonable estimate of the uncertainty is less than about three percent.

One source of error could be attributed to an uncertainty in the temperature measurement. The temperature was only recorded initially before the run started. The assumption that this temperature is representative will be reasonable if a steady state condition is initially established. Most of the measurements, however, are taken while the temperature is changing. The rate of change was less than a few degrees over the period of the test. Hence, temperature is only known within plus or minus about 2° K.

Several assumptions were made in the derivation of the solution of the partial heat equation in the preceding section of this report. At that time, the comment was made that the errors introduced by making these assumptions would be deferred to this section. These errors will be estimated here.

The sum total of all errors introduced by all of the assumptions can be estimated by noting the difference in the solution as derived previously and the exact solution. A perturbation method will be used to find an estimate of the exact solution.

The conductivity is a function of temperature. The value of the conductivity will be approximated by the first two terms of a Taylor's expansion so that

$$K \doteq K_0 (1 + \epsilon v) \qquad (40)$$

where K_0 is the conductivity at T_0 and is a constant, v_0 is the solution to the heat transfer equation where the conductivity was assumed to be constant, etc. For our particular case, the highest temperature change possible can be shown to be less than 30° K. The results in the section on MEASUREMENTS indicate that the conductivity can be approximated quite well by a linear function.

The value of ϵ is small and can be estimated by considering the theoretical temperature dependence of the conductivity as derived in the INTRODUCTION to this report. The predicted temperature dependence is

$$K = A T^3 + B . \qquad (41)$$

This expression may be expanded so that

$$K(v) \doteq K_0(1 + \epsilon v) = (A_0 T_0{}^3 + B) + 3 A T_0{}^2 v \qquad (42)$$

where K_0 and ϵ are given by

$$K_0 = A T_0{}^3 + B \qquad (43)$$

and

$$\epsilon = 3 A T_0{}^2 / K_0 . \qquad (44)$$

For this typical example

$$\epsilon \simeq 3 / T_0 .$$

The lowest temperature for which the conductivity was measured is $100°$ K so that $\epsilon \simeq 0.03$.

The quantity of interest is $\dfrac{\partial v(a, t)}{\partial t}$, which is the time rate of change of the difference in temperature located at $|\vec{r}| = a$. The partial differential heat equation must hold everywhere in the region and can be written as point a and time t as

$$\frac{\partial v(a, t)}{\partial t} = \frac{1}{\rho C} \; [K(v) \; \nabla^2 v + \nabla \; (K(v) \cdot \nabla v)] \; . \tag{45}$$

Perturbation theory considers a first-order correction to a known solution of a very similar problem. The temperature change can be represented by

$$v = v_0 + v_1 \epsilon \tag{46}$$

where ϵv_1 is the first-order correction to the known solution (v_0).

Expanding equation (45) and dropping second-order terms,

$$\frac{\partial v}{\partial t} = \frac{\partial v_0}{\partial t} + \epsilon \; \frac{\partial v_1}{\partial t}$$

$$= \frac{1}{\rho C} \; [K_0 \; \nabla^2 \; v_0 + \epsilon \; K_0 \; v_0 \; \nabla^2 \; v_0 + \epsilon \; K_0 \; (\nabla v_0)^2 + \epsilon \; K_0 \; \nabla^2 \; v_1] \tag{47}$$

The quantity that is measured at position a is $\partial v / \partial t$, and the conductivity is evaluated by considering $(\partial v / \partial t) \doteq (\partial v_0 / \partial t)$. The whole object of this exercise is to show

$$\frac{\partial v_0}{\partial t} \gg \epsilon \left(\frac{\partial v_1}{\partial t} \right) \; . \tag{48}$$

From equation (47)

$$\frac{\partial v_1}{\partial t} = k_0 \; v_0 \; \nabla^2 \; v_0 + k_0 \; (\nabla v_0)^2 + k_0 \; \nabla^2 \; v_1 \tag{49}$$

or

$$\frac{\partial v_1}{\partial t} = k_0 \; \nabla^2 \; (v_0^2/2) + k_0 \; \nabla^2 \; v_1 \; . \tag{50}$$

The first term on the right in this last equation reaches a maximum value with respect to time. Let this maximum value be represented by "M." Equation (50) becomes

$$\frac{\partial v_1}{\partial t} \leq M + k_0 \; \nabla^2 \; v_1 \tag{51}$$

or

$$\frac{\partial (v_1 - Mt)}{\partial t} \leq k_0 \; \nabla^2 (v_1) \tag{52}$$

where M is independent of time and position. At a particular time consider a constant M' so that

$$\frac{\partial (v - M't)}{\partial t} = k_0 \; \nabla^2 \; (v_1 - M't) \; . \tag{53}$$

For this time and place

$$v_1(a, t) = v_0(a, t) + M't \leq v_0(a, t) + M t \; . \tag{54}$$

Since the time picked is arbitrary, the inequality-equal statement holds for all values of time.

30

$$\frac{\partial v_1(a, t)}{\partial t} \leq k_0 \, v_0 \, \nabla^2 v_0 + k_0 (\Delta v_0)^2 + k_0 \, \nabla^2 v_0 \ . \tag{55}$$

The terms in the above equation are easily found from the expression of v_0 so that

$$\nabla \, v_0 = \left(\frac{2t}{a} \right) \left(\frac{\partial v_0}{\partial t} \right) \hat{e}_r \tag{56}$$

and

$$k_0 \, \nabla^2 v_0 = \frac{\partial v_0}{\partial t} \ . \tag{57}$$

Equation (55) can now be written as

$$\frac{\partial v_1}{\partial t} \leq v_0 \, \frac{\partial v_0}{\partial t} + \left(\frac{4 \, k_0 \, t}{a^2} \right) t \left(\frac{\partial v_0}{\partial t} \right)^2 + \left(\frac{\partial v_0}{\partial t} \right) \ . \tag{58}$$

The ratio defining E

$$E = 100 \left(\frac{\epsilon \, \dfrac{\partial v_1}{\partial t}}{\dfrac{\partial v_0}{\partial t}} \right) \tag{59}$$

is an estimate of the percent error introduced herein by the assumptions in the section METHOD OF MEASUREMENT. Using equation (58) where the second term is of the same order of magnitude as the first term,

$$E \lesssim (100) \ (0.03) \ (3 + 3 + 1) \simeq 21 \ \%. \tag{60}$$

The value for the error as expressed above is for the worst possible case. At room temperature where $\epsilon \simeq 0.01$,

$$E \lesssim 7\% \ . \tag{61}$$

The value of the conductivity changes more than an order of magnitude for the temperature range of 100° K to 500° K, as will be shown later. Errors of seven percent or even 21 percent are not very significant when considering the gross behavior. More will be said about the magnitudes of the errors and their effect on the results in the concluding section of this report.

Selection of Powder

Spherical glass beads, called micro-beads, were selected as the powder. They conform to some of the simple assumptions of the theory and are obtainable in a number of sizes. The data may also be compared with the work of other experimenters. According to the manufacturer's specification, less than one percent of the particles are sharp or angular; less than two percent show milkiness or surface scoring or scathing, and less than one-half percent any foreign matter. The beads are formed from a barium silicate glass.

MEASUREMENTS

The raw data gathered are listed in Appendixes B and C. The data essential for the calculation of the conductivity by method 1 are listed in Appendix B. Appendix C lists the data peculiar to method 2. Appendix B is arranged with respect to ascending temperature and not in the order in which the tests were made. Three particle sizes were chosen. Table I shows the relationship between the particle size and the sample number.

TABLE I. RELATIONSHIP BETWEEN PARTICLE SIZES OF
POWDER AND SAMPLE NUMBERS

Particle size microns, μ	Porosity p	Sample
10 to 20μ	0.41	7
38 to 53μ	0.38	6,8
125 to 243μ	0.50	2,3,5

The calculated conductivities are listed in Tables II through VI. Each row refers to one run. The first column is the run number and is immediately followed by the sample number. The second digit on samples 2 and 3 indicates

TABLE II. CALCULATED CONDUCTIVITIES FOR 10 TO 20μ POWDERS

| Run | No. | Temp, °K | Conductivity (10^{-5} W/cm°K) | | | Time,[a] sec |
			Method 1	Method 2	Method 3	
407	7	326	1.71	1.48	–	–
408	7	335	2.06	1.49	1.22	168
409	7	351	1.71	1.45	1.42	145
410	7	377	2.01	1.62	1.73	116.5
411	7	396	2.06	1.87	1.90	110
412	7	425	2.04	2.09	2.29	96
413	7	446	2.43	2.38	2.74	86
414	7	461	2.93	2.53	2.74	86.5
416	7	481	2.78	2.83	3.25	73.2
402	7	513	4.90	4.21	3.48	53.2
404	7	513	4.73	3.90	3.41	57

a. Time consumed after initiation of a run before reaching the second point which is equal to one-half of the maximum

a different day or similar situations. The next column lists the temperature in degrees Kelvin. The conductivity as calculated by method 1, method 2, and/or method 3 is indicated in the next three columns, respectively. Method 2 was applied to most of the runs except samples 2 and 3. The actual data reduction was performed by IBM 7040, 7094, and 1130 computers. All mathematical manipulations were of a straightforward nature; hence, they will not be reproduced here.

TABLE III. CALCULATED CONDUCTIVITIES FOR 38 TO 53μ POWDERS

Run	No.	Temp, °K	Conductivity (10^{-5} W/cm° K)	
			Method 1	Method 2
418	8	100	0.37	0.36
419	8	126	0.51	0.52
420	8	172	0.72	0.65
421	8	204	0.89	0.95
422	8	232	1.07	1.04
423	8	248	1.22	1.17
424	8	265	1.12	1.10
406	8	305	1.31	
370	6	346	1.69	1.62
372	6	363	1.96	
375	6	376	2.05	1.94
378	6	384	2.11	2.10
380	6	392	2.01	1.96
415	8	422	2.83	2.67
381	6	444	3.31	3.35
417	8	449	2.52	3.22
382	6	460	3.65	3.90
383	6	469	3.85	3.83
403	8	476	3.83	3.82
405	8	476	3.89	3.87
384	6	479	4.18	4.18
385	6	486	4.21	4.49
362	6	489	4.38	4.52
365	6	489	4.56	4.84
386	6	492	4.47	-

TABLE IV. CALCULATED CONDUCTIVITIES FOR SAMPLE NUMBERS WITH 125 TO 243μ POWDERS

Run	No.	Temp, °K	Conductivity (10^{-5} W/cm K)	
			Method 1	Method 2
389	5	103	0.17	0.17
390	5	104	0.17	0.17
391	5	107	0.18	0.18
392	5	110	0.17	0.17
393	5	115	0.18	0.18
394	5	121	0.18	0.18
395	5	131	0.23	0.24
396	5	141	0.25	0.26
397	5	150	0.28	0.29
398	5	165	0.35	0.36
399	5	177	0.46	0.47
400	5	196	0.60	0.57
401	5	208	0.65	0.62
363	5	316	1.48	1.54
364	5	323	1.48	1.62
366	5	333	1.84	1.86
367	5	351	2.14	2.23
360	5	365	2.60	2.67
368	5	365	2.60	2.57
354	5	385	2.92	2.97
355	5	385	2.84	2.93
353	5	387	3.27	3.43
369	5	388	3.39	3.42
359	5	401	3.26	3.35
387	5	406	3.16	3.23
371	5	416	4.34	5.08
373	5	425	4.82	4.59
358	5	429	4.29	4.23
374	5	433	4.94	4.86
376	5	442	5.04	4.97
356	5	444	5.22	—
357	5	445	4.85	4.96
388	5	449	5.91	6.35
377	5	459	5.89	5.62
352	5	468	5.36	5.59
379	5	478	6.59	6.74
351	5	481	5.66	5.56
350	5	485	5.85	6.04
348	5	485	5.97	5.98
349	5	485	5.85	5.85
350	5	485	5.85	6.01

TABLE V. CALCULATED CONDUCTIVITIES FOR SAMPLE NUMBER 2 WITH 125 TO 243μ POWDERS

Run	No.	Temp, °K	Conductivity (10^{-5} W/cm°K) Method 1
325	23	302	1.05
323	23	303	1.18
306	22	304	1.10
327	23	309	.97
329	23	323	1.33
331	23	335	1.45
312	22	336	1.50
333	23	348	1.61
317	22	370	2.09
319	22	374	2.18
321	22	382	2.21
291	21	402	2.55
294	21	402	2.65
300	21	402	2.55
296	21	403	2.63
298	21	403	2.75
302	21	403	2.55

The conductivity versus temperature is plotted in Figures 10 through 14. The abscissa is the absolute temperature in degrees Kelvin, and the conductivity is expressed along the ordinate in units of 10^{-5} W/cm°K. The selection of a semilog graph presentation allows all of the conductivity data for one particle size to be conveniently located on one graph. Figure 10 is a plot of the 10 to 20μ size powder conductivity data. Method 3 gives the smoothest data. The

TABLE VI. CALCULATED CONDUCTIVITIES FOR SAMPLE NUMBER 3 WITH 125 TO 243μ POWDERS

Run	No.	Temp, °K	Conductivity (10^{-5} W/cm°K) Method 1
336	35	215	0.48
339	35	215	0.49
370	35	222	0.48
340	36	223	0.54
341	36	238	0.58
342	36	255	0.67
343	36	270	0.59
335	34	301	0.99
324	33	302	1.05
326	33	302	1.01
307	32	303	1.08
309	32	305	1.08
328	33	315	1.12
311	32	327	1.17
330	33	331	1.39
332	33	341	1.35
313	32	342	1.26
315	32	351	1.40
316	32	360	1.61
334	33	358	1.55
318	32	371	1.73
320	32	377	1.89
322	32	385	1.98
397	31	401	2.14
299	31	401	2.15
301	31	401	2.15
303	31	401	2.15

maximum chart reading for these measurements was reached in a time t_m on the order of 10 seconds. This means that the uncertainty in this time is large for the usual method 1 data reduction procedure. The uncertainty explains the scatter in the data. The initial points near t_m were used by method 2.

Figure 11 is a plot of the data for the 38 to 53μ size powder. The data represented by the triangles were found in the literature [14]. Table VII gives the pertinent properties of these measurements.

TABLE VII.   GLASS BEADS, 50μ AVERAGE PARTICLE SIZE

Method	Temp, °K	Gas Pressure, torr	Conductivity, 10^{-5} W/cm°K
LHS	298	8×10^{-5}	2.5
Probe	298	5×10^{-4}	3.2
Guarded cold plate	190	2×10^{-4}	1.7

These values are greater than the other values reported. The relatively high gas pressure may have resulted in an appreciable gas conduction.

The data represented by the squares were also found in the literature [28]. These data were for 44 to 74μ glass beads at a pressure of less than 2×10^{-6} torr and were gathered by an LHS method. The system was stablized for at least 24 hours.

Figure 12 is a plot of the 125 to 243μ of sample 5 and similar sized powders recorded in the literature. The data represented by the triangles have the properties given in Table VIII [14]. The data represented by the square were also obtained from the literature [28].

TABLE VIII. 150μ AVERAGE PARTICLE SIZE

Method	Temp, °K	Gas Pressure, torr	Conductivity 10^{-5} W/cm°K
LHS	298	3×10^{-4}	5.0
Probe	298	3×10^{-5}	5.0
Guarded cold plate	190	3×10^{-4}	4.6
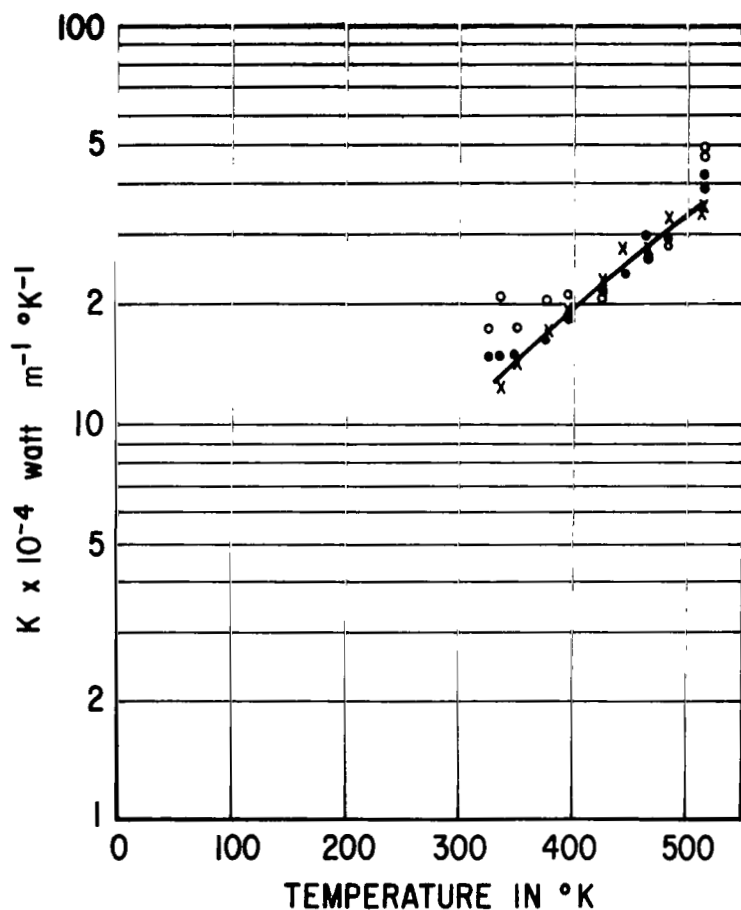
FIGURE 10. PLOT OF CONDUCTIVITY FOR 10
TO 20μ SIZE POWDER (Open circles represent
conductivity obtained by method 1, solid circles
by method 2, and crosses by method 3.)
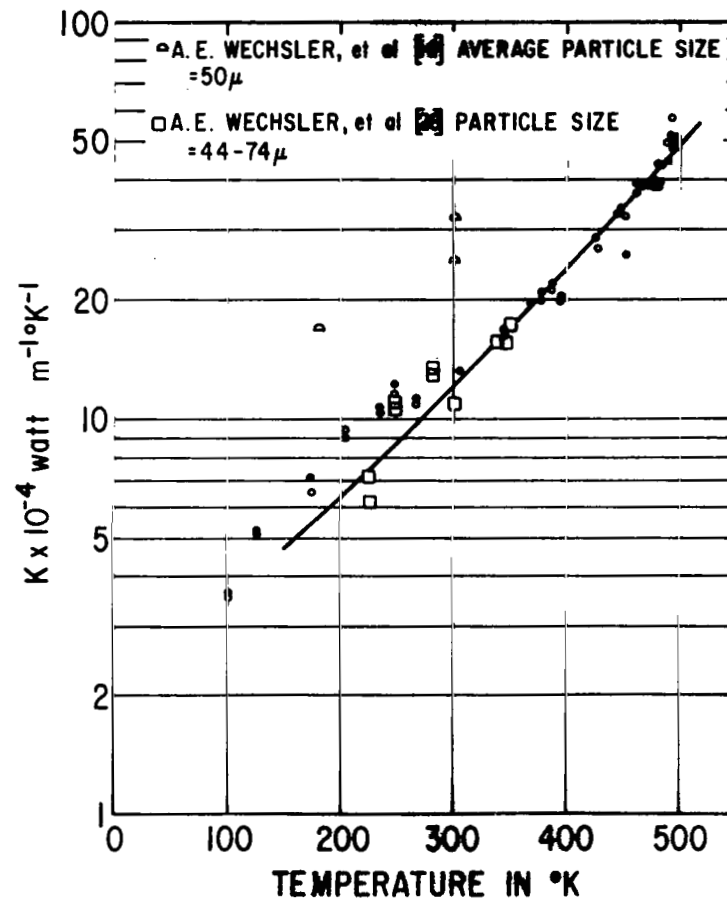
FIGURE 11. PLOT OF CONDUCTIVITY FOR 38
TO 53μ SIZE POWDER (Open circles represent
conductivity obtained by method 1 and solid
circles method 2.)
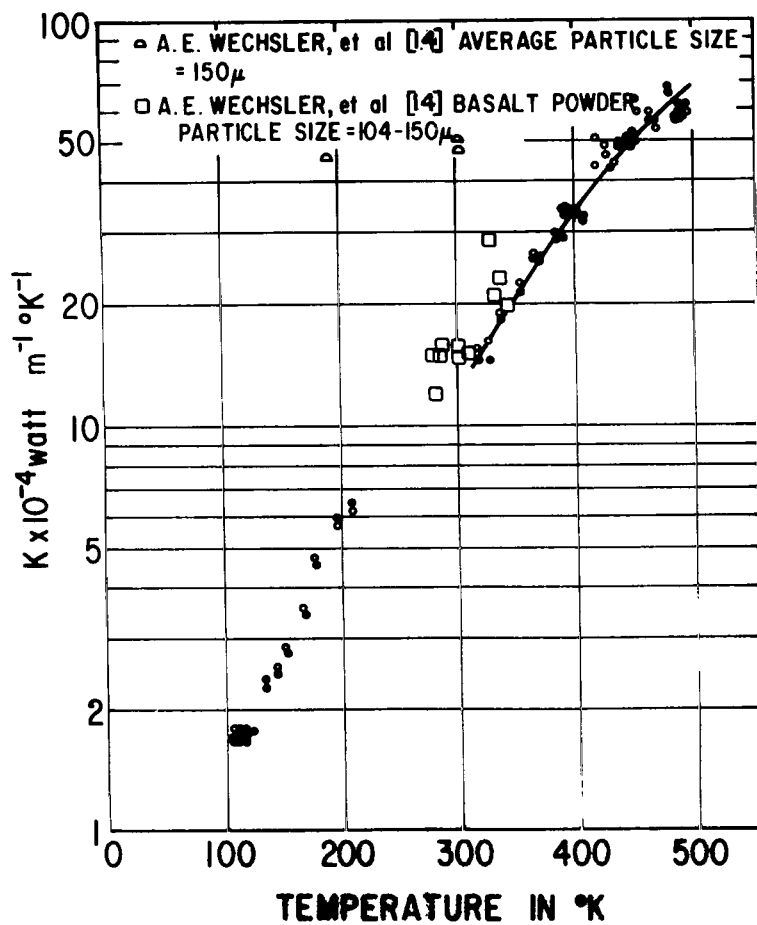
FIGURE 12. PLOT OF 125 TO 243μ SIZE POWDERS
OF SAMPLE 5 AND SIMILAR SIZE PARTICLES
FOUND IN LITERATURE (Open circles represent
conductivity obtained by method 1 and solid
circles method 2.)
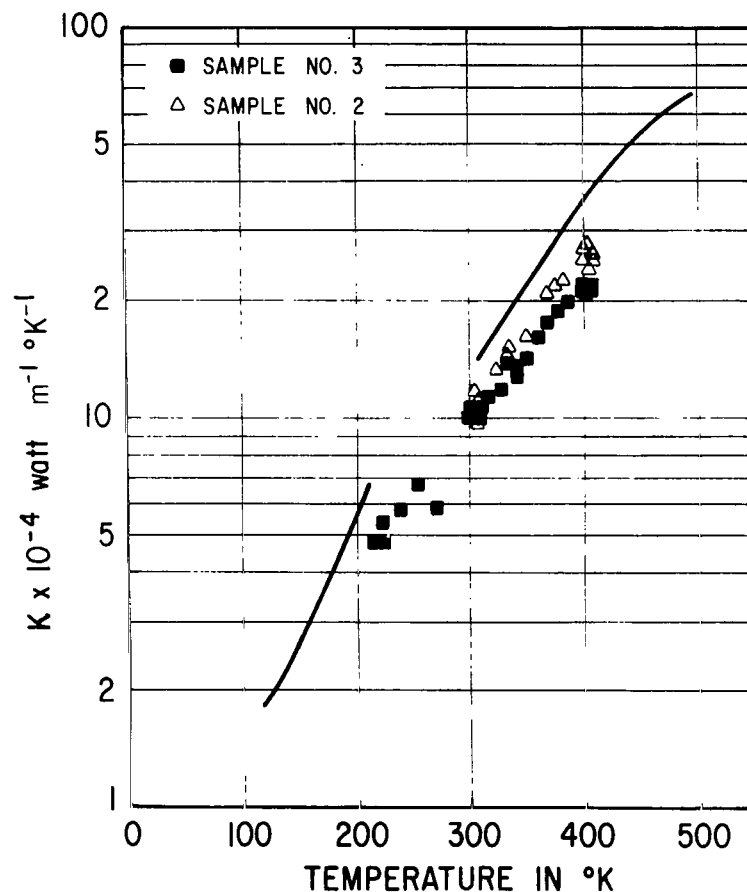
FIGURE 13. PLOT OF REMAINING 125 TO 243μ
DATA OF SAMPLES 3 AND 4

Figure 13 is a plot of the re-
maining 125 to 243μ data of samples
3 and 4. The curve in this diagram
describes the data of sample 5. Fig-
ure 14 is a composite of Figures 10,
11, and 12, where the lines represent
the data points.
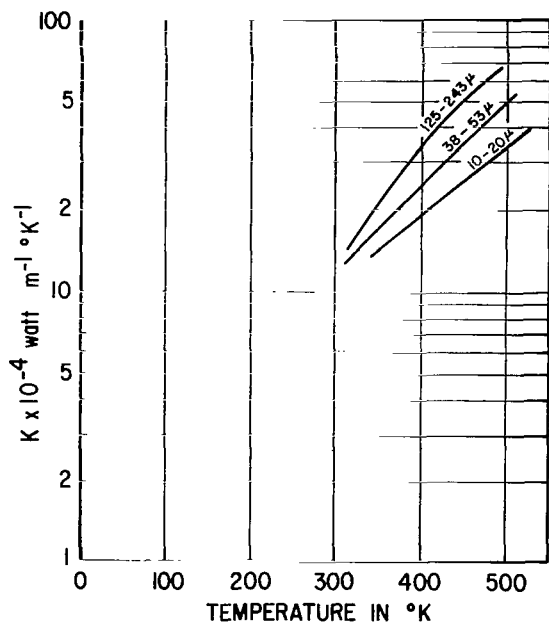
FIGURE 14. COMPOSITE OF
FIGURES 10, 11, AND 12 WITH
LINES REPRESENTING DATA
POINTS

CONCLUSIONS

Discussion

Three ways of calculating the
conductivity were presented in the
preceding section of this report. The
accuracy of each depends on a number
of factors. From a statistical stand-
point the greater the number of data
points used, the more accurate the
conductivity. The least square
method (method 2) uses many more
points than the other methods and should be more accurate. Each data point
should be weighted statistically according to its significance.

Method 2 gives nearly the same results as the numerically simpler
methods of using the halfway points of the maximum on the chart recording,
as in methods 1 and 3. Using the first halfway point (method 1) is useful
because the length of the run is shorter, and hence the uniform rate of change
of the temperature, which is initially determined, need hold for a shorter length
of time when compared to method 3. Method 3 becomes more useful, however,
when the uncertainty in the first halfway point becomes unacceptable as demon-
strated by the conductivity data of the 10 to 20μ powder. Except for this case,
the conductivity data found through method 1 is used throughout the remainder
of this chapter.

Two equations were tested to see which best describes conductivity as
a function of temperature. Equation (62) is equivalent to equations (8), (9),
and (10). In these equations, all of the quantities except perhaps the intrinsic

solid conductivity K_{sol} are independent of temperature. The total conductivity can then be written as some constant times K_{sol} plus another constant times the temperature to the third power. Values for K_{sol} as a function of temperature for the particular glass could not be found in the literature. The conductivity does, however, have nearly the same temperature dependence as its heat capacity [34]. Values for the heat capacity were found in the literature between 300° to 500° K [35] and were measured between 200° to 300° K and extrapolated from 200 to 100° K. A sixth-order polynomial was fitted to the heat capacity data by the least squares method. The first equation can now be written in terms of heat capacity where

$$K = E \, C(T) + DT^3 \; . \tag{62}$$

Watson made the approximation that K_{sol} is nearly independent of temperature [36]. The second equation corresponds to this approximation so that

$$K = AT^3 + B \; . \tag{63}$$

Equations of the form of equations (62) and (63) were fitted to the conductivity versus temperature data by the least square method. The values of A, B, D and E are presented in Table IX. Some of the conductivity data appear disjointed between 200° and 300° K. Separate calculations were made for all of the data below and above 300° K. The quantity represented by f is the sum of the squares of the deviation and is a measure of how well the curve fits the data. The values of f are slightly lower for equation (63).

For the 10 to 20μ powder the curves of the form of equations (62) and (63) are practically indistinguishable over the range of the data. These curves are represented by a single line in Figure 15.

Figure 16 represents the comparison between the experimental data for the 38 to 53μ range powder and equation (62). The lower curve is the best fit for all data above 300° K. Figure 17 shows the fit of equation (63). Figure 18 is a plot of equations (62) and (63) and the data on a Cartesian coordinate system. The discrepancy between the data points and the curves is not as apparent at the lower conductivity values as with the semilog graphs.

42

TABLE IX.   VALUES OF CONSTANTS A, B, D, AND E FOUND BY LEAST SQUARE METHOD

Particle Size	Sample	Method of Data Reduction	No. of Experiments	$W\,M^{-1}{}^{\circ}K^{-1}$ E $\times 10^{-3}$	$W\,M^{-1}{}^{\circ}K^{-4}$ D $\times 10^{-10}$	f-I	$W\,M^{-1}{}^{\circ}K$ B $\times 10^{-3}$	$W\,M^{-1}{}^{\circ}K^{4}$ A $\times 10^{-10}$	f-II
10 to 20μ [a]	7	3	11	0.662	0.209	0.0139	0.484	0.230	0.0155
10 to 20μ [a]	7	2	11	0.433	0.241	0.0585	0.346	0.252	0.0556
10 to 20μ [a]	7	1	11	0.572	0.264	0.221	0.472	0.276	0.213
38 to 53μ [a]	6,8	1	24	0.759	0.292	0.0351	0.454	0.327	0.0241
38 to 53μ [b]	6,8	1	17	0.196	0.353	0.0147	0.153	0.358	0.0143
38 to 53μ [c]	6,8	1	7	1.36	0.153	0.0035	0.437	0.452	0.0083
125 to 243μ [a]	5	1	41	0.103	0.538	0.108	0.071	0.542	0.107
125 to 243μ [b]	5	1	28	-0.140	0.566	0.152	-0.132	0.565	0.151
125 to 243μ [c]	5	1	13	0.295	0.545	0.00044	0.0870	0.639	0.00034
125 to 243μ [a]	3	1	27	0.264	0.293	0.0039	0.151	0.310	0.0037
125 to 243μ [a]	2	1	17	-0.144	0.424	0.00523	-0.093	0.417	0.00522

a. All the data points used in computing the values

b. All the data points above 300°K used in computing the values

c. All the data points below 300°K used in computing the values

Figures 19 and 20 are comparisons of the 125 to 243μ data of sample 5. Again equation (63) appears slightly more representative. Samples 2 and 3 had fewer data points and were not spread over as wide a temperature range as sample 5; hence, less significance is associated with the values of their constants A, B, D, and E. Figure 21 depicts the fit for these two samples.

Table IX and Figures 15 through 21 show Watson's equation fitting the data slightly better than equation (62). The difference, however, is small. The values of B in Table IX were compared to Watson's values in Figure 22 [21]. His values are bounded by the rectangles enclosing the dotted-in area. The data of this report are represented by the thatched-in rectangle. The vertical span of the rectangle represents a two-standard deviation range in B or one-standard deviation from the mean in each direction. The horizontal span represents the particle size distribution. Both sets of data agree within experimental error.

Figure 23 compares the values of A with Watson's values [21]. His values are correspondingly larger for each measured particle size. The labeled lines describe the limits of the calculated values as expressed by the equations of Wesselink and Laubitz. The limits are determined by the range of porosity. The expression developed by Schotte is independent of porosity and expresses the measured data, as reported here, better than any of the other expressions.

The possibility exists of the particles not being completely opaque. The mean free path is given by Λ where

$$\Lambda = \frac{3A}{16\sigma}$$

as can be shown from equation (6). Table X shows the relationship between the particle size, the value of A, and the mean free path (Λ).

TABLE X. MEAN FREE PATH

Particle Size, μ	$A \times 10^{-10}$ W M^{-1} °K^{-1}	$\sigma_A \times 10^{-10}$ W M^{-1} °K^{-1}	Λ, μ	σ_Λ, μ
10 to 20	0.276	0.097	91.3	32
38 to 53	0.327	0.034	108	11
125 to 243	0.405	0.043	134	14
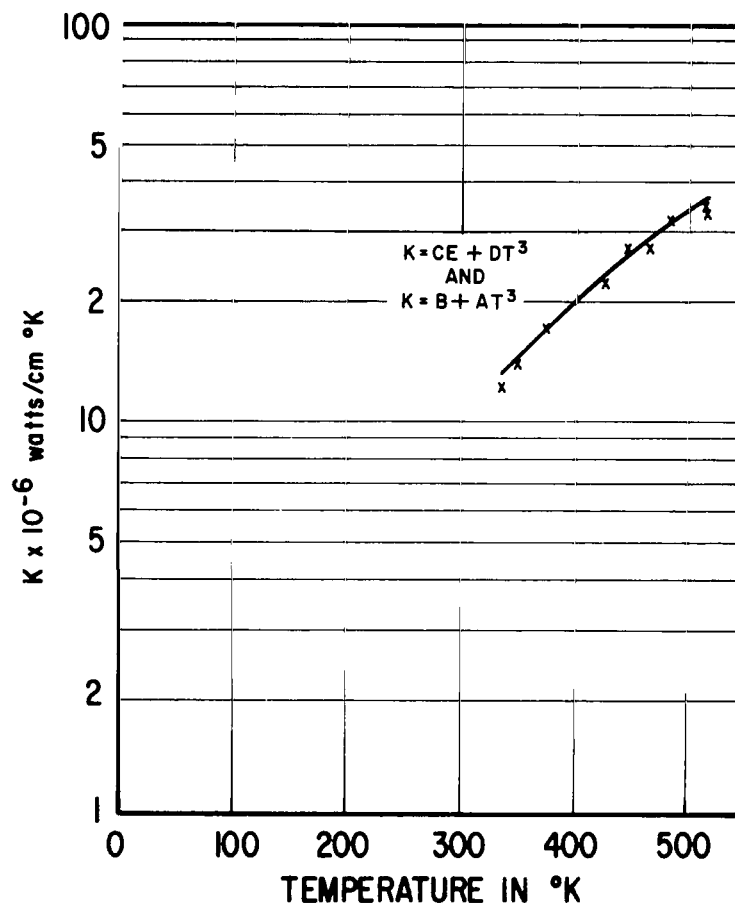
FIGURE 15. COMPARISON BETWEEN LEAST
SQUARE CURVES AND 10 TO 20μ POWDER
DATA. (The crosses represent the data obtained
by method 3. The curve represents both solutions
of equation (1) and equation (2).)
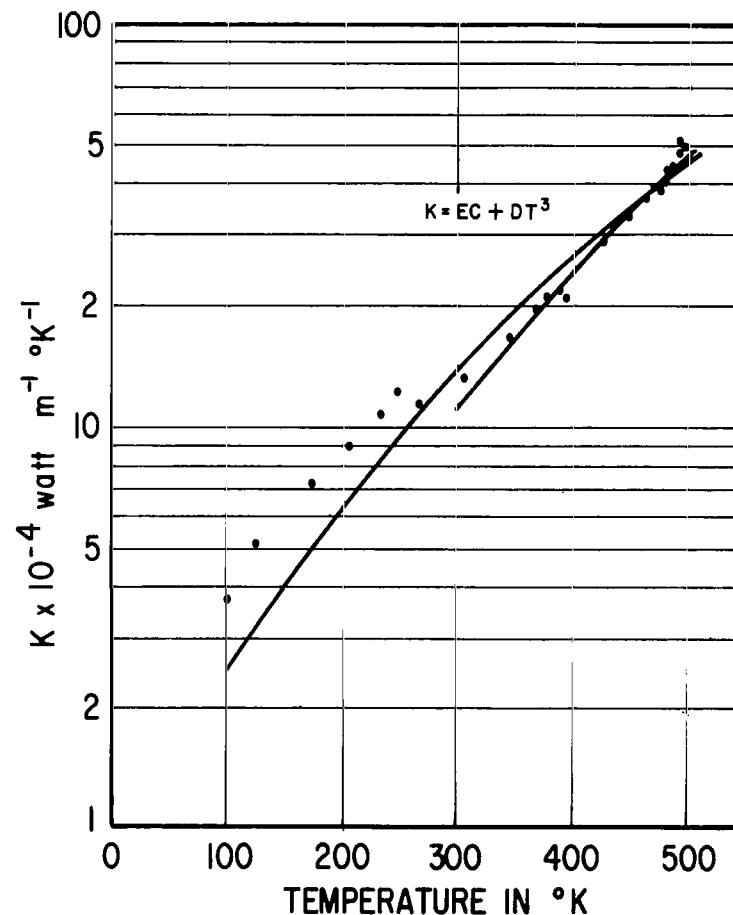
FIGURE 16. COMPARISON BETWEEN LEAST
SQUARE FIT OF EQUATION (1) AND DATA
FOR 38 TO 53μ POWDER
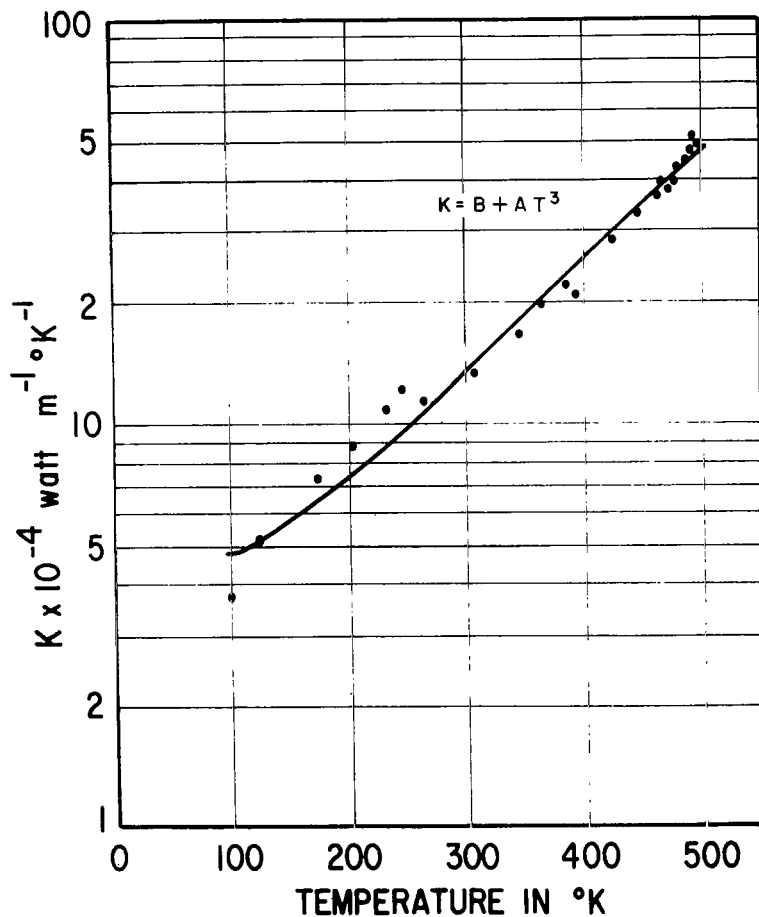
FIGURE 17. COMPARISON BETWEEN LEAST
SQUARE FIT OF EQUATION (2) AND DATA
FOR 38 TO 53μ POWDER
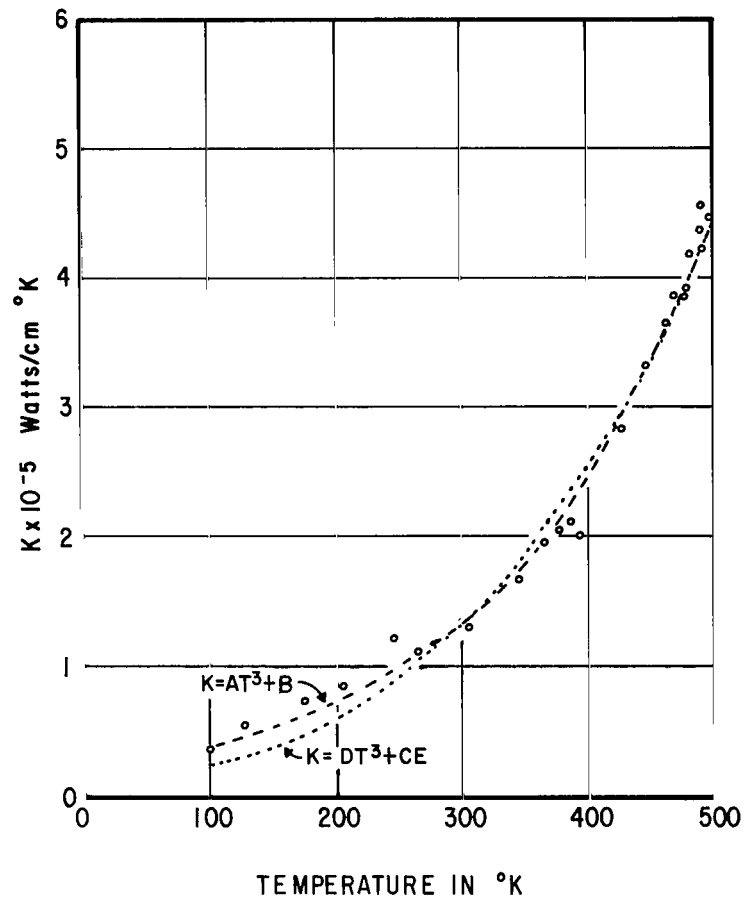
FIGURE 18. COMPARISON OF LEAST SQUARE
FITS OF EQUATIONS (1) AND (2) WITH DATA
FOR 38 TO 53μ RANGE PLOTTED ON
CARTESIAN COORDINATE SYSTEM
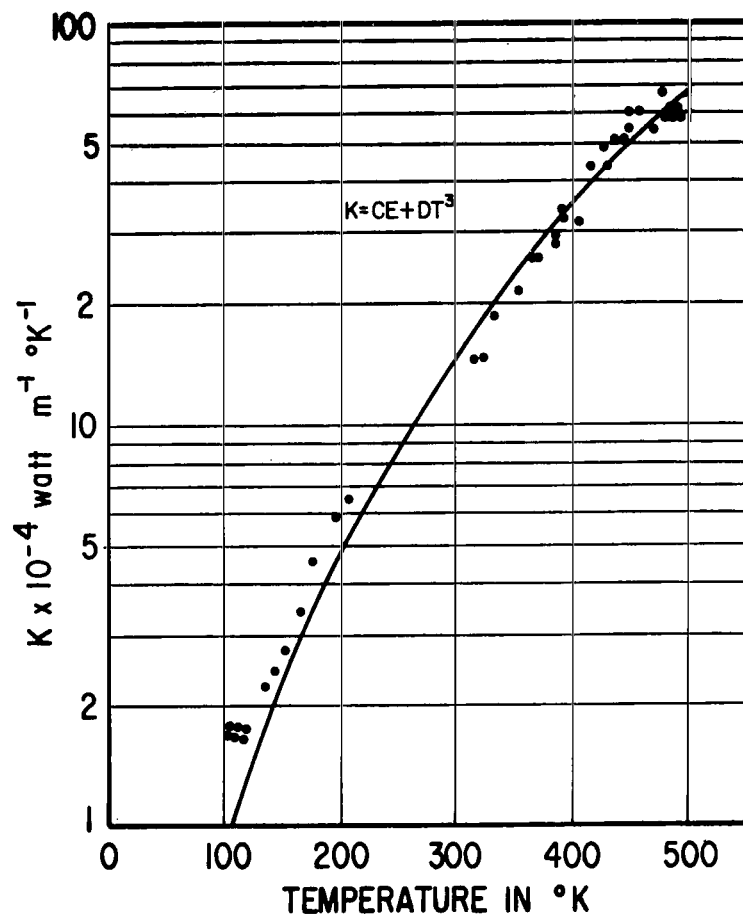
FIGURE 19. COMPARISON OF LEAST SQUARE
FIT OF EQUATION (1) WITH DATA FOR
125 TO 243μ POWDER
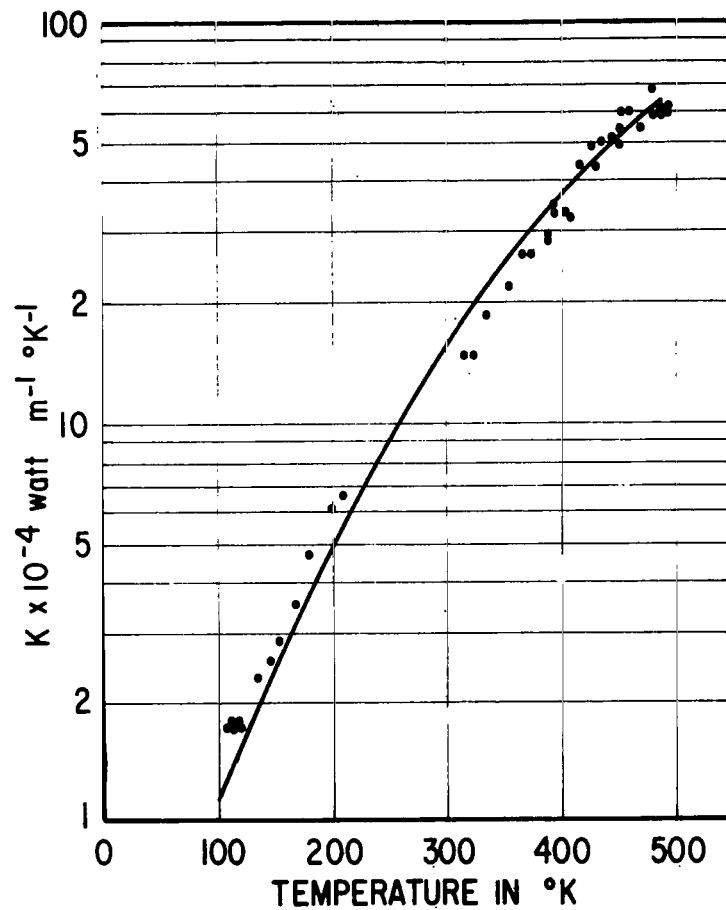
FIGURE 20. COMPARISON OF LEAST SQUARE
FIT OF EQUATION (2) WITH DATA FOR
125 TO 243μ POWDER

47
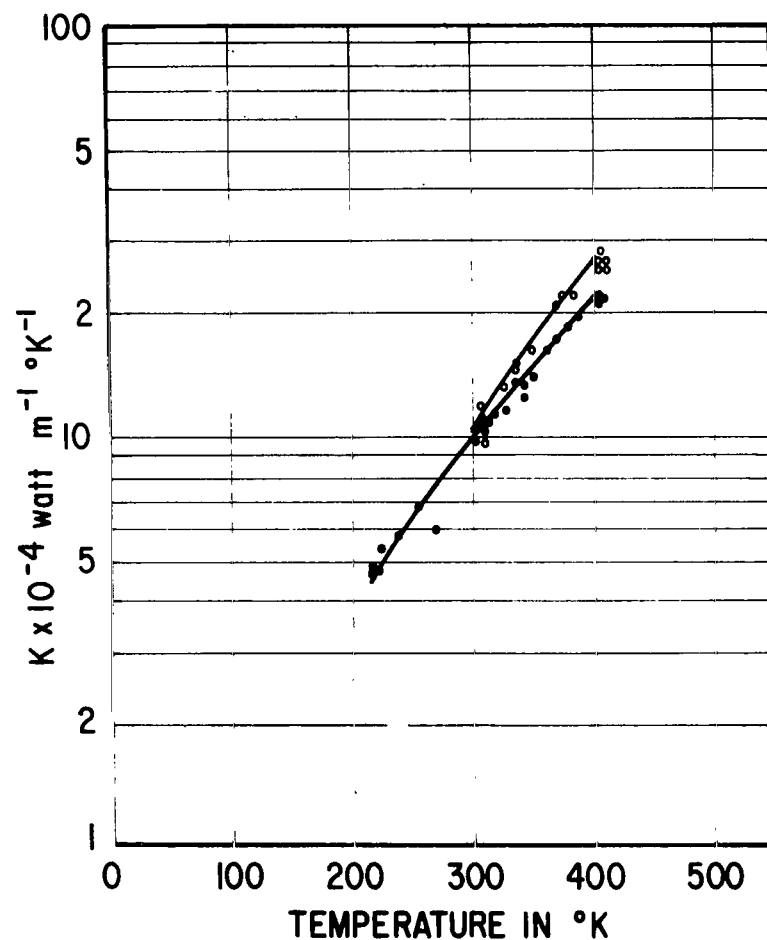
FIGURE 21. COMPARISON OF LEAST SQUARE
FITS WITH DATA FOR 125 TO 243μ POWDER OF
SAMPLES 2 AND 3. (The curves of equations (1)
and (2) are practically indistinguishable over the
range of the data. The curves are represented
by a single line.)
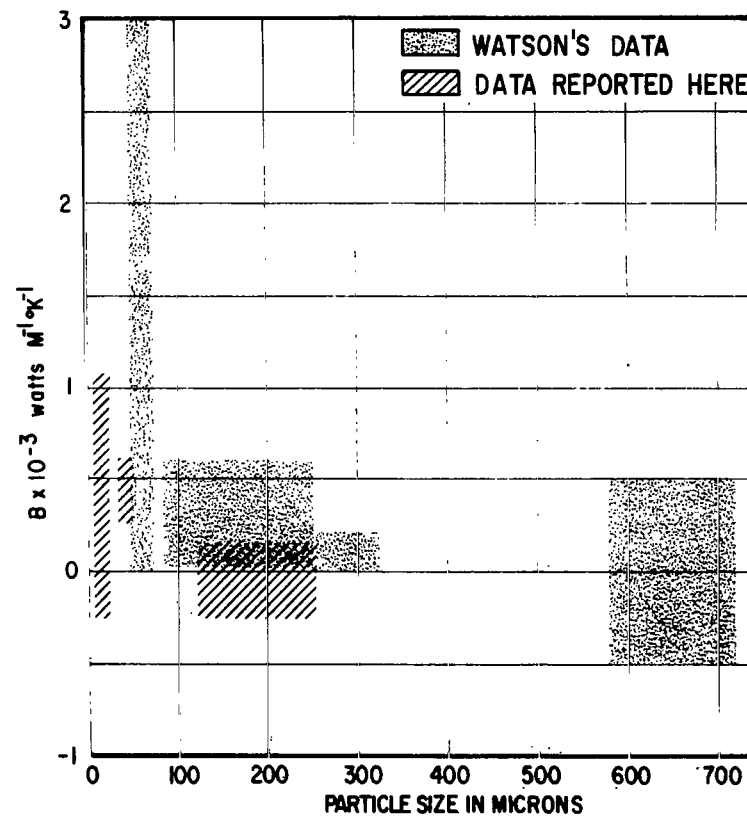
FIGURE 22. VALUES OF B IN EQUATION
$K = AT^3 + B$
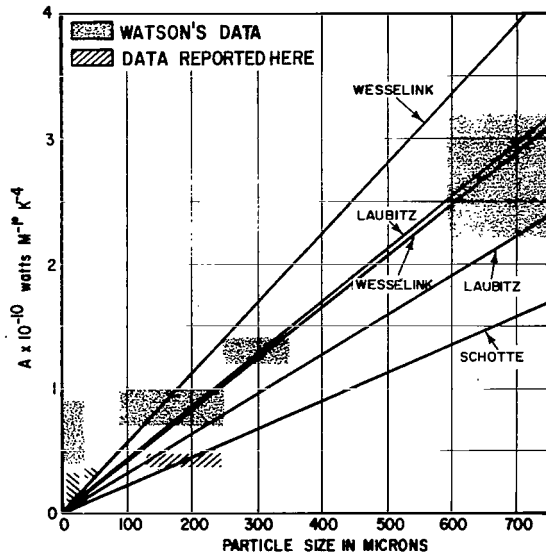
FIGURE 23. VALUES OF A IN
EQUATION K = AT³ + B

recorded in Table XI.

The values for Λ in Table X demonstrate that the powder is transparent for the 10 to 20μ and 38 to 53μ powder.

Since the mean free path (Λ) may be temperature dependent, the conductivity may not behave exactly as described by equation (63). One way to test how well this equation holds is to consider

$$K = AT^x + B \qquad (64)$$

where A, x, and B are now the parameters to be found by the least square method. A least square adjustment of the parameters was performed, and the results are

TABLE XI. VALUE FOR EXPONENT

Particle Size	Sample	x	One Standard Deviation
10 to 20μ	7	2.45	1.39
38 to 53μ	6,8	3.59	0.22
125 to 243μ	5	3.11	0.20
125 to 243μ	3	3.18	0.26
125 to 243μ	2	2.68	0.89

All values of x are within one standard deviation of x equals three except the 38 to 53μ powder. The value of x for the 10 to 20μ powder is comparatively uncertain. This means that the radiative conductivity may not totally behave as T³ but may behave slightly different for the 10 to 20μ and 38 to 53μ powders. If the absorption coefficients were known, this different behavior could be calculated as outlined in the INTRODUCTION. The conductivity for the 125 to 243μ powder apparently behaves very much like the T³ dependency. This should be expected because the particles in this size powder are opaque.

49

Summary

A method of measuring the thermal conductivity has been developed that is quite suitable for measuring evacuated powders. This method gives consistent results. It is fast, and simple initial and boundary conditions are feasible. The temperature dispersion during any one measurement is small enough to make measurements as a function of temperature meaningful.

The conductivity was measured for glass beads in a vacuum of at least 2×10^{-6} torr or better over a temperature range of 100° to 500°K. The particle sizes used were 10 to 20μ, 38 to 53μ, and 125 to 243μ. The conductivity can be represented by an expression of $K = AT^3 + B$ where A and B are constants. This result has one of two consequences. One is that the model used to develop the mathematical expression for the nonradiative component of heat transfer, as given in equation (62), may not be sufficiently descriptive. The other is that the heat capacity is not as strongly dependent on temperature as reported in the literature.

The value of A does not change significantly over the range in powder sizes from 10 to 243μ. This means that the value of A is not adequately described for these particle sizes by the theories of Wesselink, Laubitz, and Russell. Laubitz's expression is more descriptive when Watson's data are considered.

Particle sizes of 100μ or less begin to become transparent to the thermal radiation in the temperature range considered here. For this case, a simple model is sufficient to account for the behavior by considering the mean free path length (Λ) of a photon.

A comparison between Watson's data and the data reported here is difficult. Watson's data include a wide range of porosity. The porosities for the data reported here are approximately the same.

For an equal number of measurements, the determined values of A and B should be comparable. One obvious advantage to the approach followed here is that the measured temperature dependence can be displayed. Watson only determined the constants A and B.

Recommendations

Further measurements and analysis of the constants A and B would be desirable. This measurement can be performed in two ways. It can be performed through the steady state method of Watson now that the conductivity has been shown to be of the form $K = AT^3 + B$. This method is only appropriate when this equation holds. Another way would be to use the differentiated line heater source method as described previously. At high temperatures, such as 500° K, the solid conduction component is negligible. At low temperatures, such as 100° K, both the radiative and solid components are comparable; hence, from two measurements, one at high and one at low temperatures, these constants could be determined.

George C. Marshall Space Flight Center
National Aeronautics and Space Administration
Huntsville, Alabama, August 8, 1968
908-20-02-00-62

APPENDIX A

RELATIVE SIZES OF TERMS IN HEAT-TRANSFER EQUATIONS

The equation that is being considered from the section METHOD OF MEASUREMENT expresses the temperature change

$$v(a,t) = \left(\frac{F}{4\pi K}\right) \int_x^\infty \left(\frac{1}{x'}\right) \exp(-x') \, dx'$$

$$- \int_x^\infty v(b,t) \left(\frac{b}{a}\right) \exp(-x') \, dx' \tag{A1}$$

as a sum of two functions. The problem is to show the second one is small compared to the first.

The absolute value of the second term is considered where

$$\left| \int_x^\infty v_b \left(\frac{b}{a}\right) \exp(-x') \, dx' \right| \leq \left| v_{bmax} \left(\frac{b}{a}\right) \exp(-x) \right| \tag{A2}$$

which is less than or equal to $\left| v_{bmax} \dfrac{b}{a} \right|$ where $x \geq 0$.

Physically this means that the maximum temperature of the heater wire during a test times the ratio (b/a) is always greater than the second term in equation (A1). The temperature change of the heater wire (v_b) can be found by considering the heater wire as an isolated probe. Calculations show that the heater wire exceeded the temperature of the thermocouple by a factor of 20 or less. The maximum temperature change is at the time t as used in equation (A1). For the particular geometry and construction used, $b = 5 \times 10^{-4}$ inches and $a \simeq 2 \times 10^{-2}$ inches so that the value of the inequality in equation (A2) becomes

$$\left| v(b,t) \left(\frac{b}{a}\right) \right| \geq \left| 20 \, v(a,t) \, \frac{b}{a} \right| \simeq 0.5\% \, v(a,t) \tag{A3}$$

By noting equation (A1) the second term is obviously small in comparison by a factor of 0.5 percent or less.

APPENDIX B

DATA LISTING FOR CONDUCTIVITY CALCULATIONS

Included in this appendix are all of the data needed to calculate the conductivity by method 1. Each row is one measurement. The first column labeled RUN NO is the run number and the sample number. The first three-letter number is the run number. The first digit of the second number is the sample number and the second digit, if there is one, refers to succeeding days. The column labeled TEMP is a listing of the temperature in degrees Kelvin. The next column is a listing of the time at which half of the maximum is reached on the chart record. The chart reading in the range of zero to 100 is recorded in the next column in decivolts. The other values are explained in the text. The vacuum pressure during all measurements was 2×10^{-6} torr or better. The measurements are listed according to ascending temperature and not according to the run number or the chronological order in which they were taken.

LISTING OF RAW DATA

RUN NO		TEMP	TIME(1/2) IN SEC.	ECM SCALE RE.	SWITCHES S1	S2	V IN VOLTS	I IN MLAMPS	L IN CM	DENSITY GM/CM**3
407	7	326	9.8	71.0	500	1000	1.69	12.2	13.68	1.21
408	7	325	8.7	67.0	500	1000	1.69	12.2	13.68	1.21
409	7	351	10.4	68.0	500	1000	1.69	12.2	13.68	1.21
410	7	377	8.7	35.0	1000	1000	1.69	12.2	13.68	1.21
411	7	396	9.8	34.0	1000	1000	1.69	12.2	13.68	1.21
412	7	425	9.5	32.0	1000	1000	1.69	12.2	13.68	1.21
413	7	446	8.4	61.0	500	1000	1.69	12.2	13.68	1.21
414	7	461	7.0	61.0	500	1000	1.69	12.2	13.68	1.21
416	7	481	7.4	61.0	500	1000	1.69	12.2	13.68	1.21
402	7	513	3.3	79.0	500	1000	1.69	12.2	13.68	1.21
404	7	513	3.6	75.0	500	1000	1.69	12.2	13.68	1.21

LISTING OF RAW DATA

RUN NO		TEMP	TIME(1/2) IN SEC.	ECM SCALE RE.	SWITCHES S1	S2	V IN VOLTS	I IN MLAMPS	L IN CM	DENSITY GM/CM**3
418	8	100	199.0	45.0	500	200	1.48	12.4	11.63	1.13
419	8	126	168.0	46.0	500	200	1.48	12.4	11.63	1.13
420	8	172	180.0	37.0	500	200	1.48	12.4	11.63	1.13
421	8	204	165.0	36.0	500	200	1.48	12.4	11.63	1.13
422	8	232	153.0	34.0	500	200	1.48	12.4	11.63	1.13
423	8	248	142.0	33.0	500	200	1.48	12.4	11.63	1.13
424	8	265	154.0	34.0	500	200	1.48	12.4	11.63	1.13
406	8	305	157.9	59.0	500	100	1.48	12.4	11.63	1.13
370	6	346	69.0	54.0	500	200	1.46	12.4	11.52	1.13
372	6	363	62.2	52.0	500	200	1.46	12.4	11.52	1.13
375	6	376	60.0	52.0	500	200	1.46	12.4	11.52	1.13
378	6	384	57.3	53.0	500	200	1.46	12.4	11.52	1.13
380	6	392	55.2	58.0	500	200	1.46	12.4	11.52	1.13
415	8	422	82.0	28.0	500	200	1.48	12.4	11.63	1.13
381	6	444	38.5	51.0	500	200	1.46	12.4	11.52	1.13
417	8	449	74.0	35.0	500	200	1.48	12.4	11.63	1.13
382	6	460	35.0	51.0	500	200	1.46	12.4	11.52	1.13
383	6	469	33.3	51.0	500	200	1.46	12.4	11.52	1.13
403	8	476	70.0	49.0	500	100	1.48	12.4	11.63	1.13
405	8	476	70.3	48.0	500	100	1.48	12.4	11.63	1.13
384	6	479	30.7	51.0	500	200	1.46	12.4	11.52	1.13
385	6	486	30.0	52.0	500	200	1.46	12.4	11.52	1.13
362	6	489	27.8	54.0	500	200	1.46	12.4	11.52	1.13
365	6	489	27.2	52.0	500	200	1.46	12.4	11.52	1.13
386	6	492	27.2	52.0	500	200	1.46	12.4	11.52	1.13

LISTING OF RAW DATA

RUN NO		TEMP	TIME(1/2) IN SEC.	ECM SCALE RE.	SWITCHES S1	S2	V IN VOLTS	I IN MLAMPS	L IN CM	DENSITY GM/CM**3
325	23	302	44.6	64.0	200	1000	1.70	12.4	13.57	1.49
323	23	303	41.0	62.0	200	1000	1.70	12.4	13.57	1.49
306	22	304	41.0	67.0	200	1000	1.70	12.4	13.57	1.49
327	23	309	45.8	68.0	200	1000	1.70	12.4	13.57	1.49
329	23	323	37.7	61.0	200	1000	1.70	12.4	13.57	1.49
331	23	335	36.0	59.0	200	1000	1.70	12.4	13.57	1.49
312	22	336	35.0	59.0	200	1000	1.70	12.4	13.57	1.49
333	23	348	34.3	56.5	200	1000	1.70	12.4	13.57	1.49
317	22	370	29.0	52.0	200	1000	1.70	12.4	13.57	1.49
319	22	374	28.4	51.0	200	1000	1.70	12.4	13.57	1.49
321	22	382	27.5	52.0	200	1000	1.70	12.4	13.57	1.49
291	21	402	25.5	53.0	100	1000	1.25	9.1	13.57	1.49
294	21	402	25.0	52.0	100	1000	1.25	9.1	13.57	1.49
300	21	402	26.0	48.0	200	1000	1.70	12.4	13.57	1.49
296	21	403	25.0	48.5	200	1000	1.70	12.4	13.57	1.49
298	21	403	25.0	46.3	200	1000	1.70	12.4	13.57	1.49
302	21	403	26.0	48.0	200	1000	1.70	12.4	13.57	1.49
336	35	215	146.0	30.5	500	500	1.46	12.4	11.52	1.49
339	35	215	141.0	30.8	500	500	1.46	12.4	11.52	1.49
337	35	222	150.0	30.0	500	500	1.46	12.4	11.52	1.49
340	36	223	142.0	28.5	500	500	1.46	12.4	11.52	1.49
341	36	238	142.0	27.0	500	500	1.46	12.4	11.52	1.49
342	36	255	130.0	26.5	500	500	1.46	12.4	11.52	1.49
343	36	270	133.0	30.0	500	500	1.46	12.4	11.52	1.49
335	34	301	93.0	26.5	500	500	1.46	12.4	11.52	1.49

LISTING OF RAW DATA

RUN NO		TEMP	TIME(1/2) IN SEC.	ECM SCALE RE.	SWITCHES S1	SWITCHES S2	V IN VOLTS	I IN MLAMPS	L IN CM	DENSITY GM/CM**3
324	33	302	86.0	27.0	500	500	1.46	12.4	11.52	1.49
326	33	302	94.0	25.5	500	500	1.46	12.4	11.52	1.49
307	32	303	87.0	25.8	500	500	1.46	12.4	11.52	1.49
309	32	305	88.5	25.6	500	500	1.46	12.4	11.52	1.49
328	33	315	88.0	25.0	500	500	1.46	12.4	11.52	1.49
311	32	327	83.0	25.6	500	500	1.46	12.4	11.52	1.49
330	33	331	73.0	24.5	500	500	1.46	12.4	11.52	1.49
332	33	341	73.0	25.5	500	500	1.46	12.4	11.52	1.49
313	32	342	66.5	30.0	500	500	1.46	12.4	11.52	1.49
315	32	351	72.0	25.0	500	500	1.46	12.4	11.52	1.49
316	32	360	67.0	23.5	500	500	1.46	12.4	11.52	1.49
334	33	358	62.8	26.0	500	500	1.46	12.4	11.52	1.49
318	32	371	64.0	23.0	500	500	1.46	12.4	11.52	1.49
320	32	377	60.0	22.5	500	500	1.46	12.4	11.52	1.49
322	32	385	59.0	22.3	500	500	1.46	12.4	11.52	1.49
297	31	401	56.0	21.5	500	500	1.46	12.4	11.52	1.49
299	31	401	57.0	21.0	500	500	1.46	12.4	11.52	1.49
301	31	401	57.0	21.0	500	500	1.46	12.4	11.52	1.49
303	31	401	57.0	21.0	500	500	1.46	12.4	11.52	1.49

LISTING OF RAW DATA

RUN NO		TEMP	TIME(1/2) IN SEC.	ECM SCALE RE.	SWITCHES S1	S2	V IN VOLTS	I IN MLAMPS	L IN CM	DENSITY GM/CM**3
389	5	103	96.8	80.0	500	500	1.70	12.2	13.57	1.49
390	5	104	96.6	80.0	500	500	1.70	12.2	13.57	1.49
391	5	107	79.0	95.0	500	500	1.70	12.2	13.57	1.49
392	5	110	85.0	48.0	500	1000	1.70	12.2	13.57	1.49
393	5	115	79.0	50.0	500	1000	1.70	12.2	13.57	1.49
394	5	121	80.0	51.0	500	1000	1.70	12.2	13.57	1.49
395	5	131	67.0	51.0	500	1000	1.70	12.2	13.57	1.49
396	5	141	62.0	53.0	500	1000	1.70	12.2	13.57	1.49
397	5	150	58.3	53.0	500	1000	1.70	12.2	13.57	1.49
398	5	165	51.7	51.0	500	1000	1.70	12.2	13.57	1.49
399	5	177	40.0	51.0	500	1000	1.70	12.2	13.57	1.49
400	5	196	32.0	52.0	500	1000	1.70	12.2	13.57	1.49
401	5	208	31.2	51.0	500	1000	1.70	12.2	13.57	1.49
363	5	316	54.3	74.0	500	200	1.70	12.1	13.57	1.49
364	5	323	53.7	75.0	500	200	1.70	12.1	13.57	1.49
366	5	333	44.2	74.0	500	200	1.70	12.1	13.57	1.49
367	5	351	36.0	79.0	500	200	1.70	12.1	13.57	1.49
360	5	365	31.0	38.0	1000	200	1.70	12.1	13.57	1.49
368	5	365	29.0	82.0	500	200	1.70	12.2	13.57	1.49
354	5	385	27.9	76.0	500	200	1.70	12.1	13.57	1.49
355	5	385	27.9	39.0	1000	200	1.70	12.1	13.57	1.49
353	5	387	24.9	38.0	1000	200	1.70	12.1	13.57	1.49
369	5	388	20.2	91.0	500	200	1.70	12.2	13.57	1.49
359	5	401	24.4	39.0	1000	200	1.70	12.1	13.57	1.49
387	5	406	24.8	40.0	1000	200	1.70	12.2	13.57	1.49

LISTING OF RAW DATA

RUN NO		TEMP	TIME(1/2) IN SEC.	FCV SCALE RE.	SWITCHES S1	S2	V IN VOLTS	I IN MLAMPS	L IN CM	DENSITY GM/CM**3
371	5	416	15.4	47.0	1000	200	1.70	12.2	13.57	1.49
373	5	425	14.2	46.0	1000	200	1.70	12.2	13.57	1.49
358	5	429	19.2	38.0	1000	200	1.70	12.1	13.57	1.49
374	5	433	14.2	45.0	1000	200	1.70	12.2	13.57	1.49
376	5	442	12.8	49.0	1000	200	1.70	12.2	13.57	1.49
356	5	444	15.0	40.0	1000	200	1.70	12.1	13.57	1.49
357	5	445	15.4	84.0	500	200	1.70	12.1	13.57	1.49
388	5	449	11.9	45.0	1000	200	1.70	12.2	13.57	1.49
377	5	459	11.2	48.0	1000	200	1.70	12.2	13.57	1.49
352	5	468	12.0	49.0	1000	200	1.70	12.1	13.57	1.49
379	5	478	10.5	46.0	1000	200	1.70	12.2	13.57	1.49
351	5	481	11.4	49.0	1000	200	1.70	12.1	13.57	1.49
350	5	485	10.4	52.0	1000	200	1.70	12.1	13.57	1.49
348	5	485	11.4	93.0	500	200	1.70	12.1	13.57	1.49
349	5	485	10.6	51.0	1000	200	1.70	12.1	13.57	1.49
350	5	485	10.4	52.0	1000	200	1.70	12.1	13.57	1.49

APPENDIX C

DATA LISTING OF VOLTAGE VERSUS TIME

This appendix contains the data which are peculiar to method 2 where time versus chart readings are fitted to the theoretical equations giving the conductivity. The first column gives the run number. The succeeding numbers give the time in seconds versus chart reading in centivolts.

LISTING OF RAW DATA OF TIME VRS CHART READING/

RUN NO	TIME	ER	TIME	ER	TIME	ER	TIME	ER	TIME	ER	TIME	ER	TIME	ER
348	5.	5.	10.	37.	15.	66.	20.	83.	25.	91.	30.	94.	35.	92.
	40.	91.	45.	87.	50.	82.								
349	5.	5.	10.	23.	15.	38.	20.	47.	25.	51.	30.	51.	35.	50.
	40.	48.												
350	5.	5.	10.	25.	15.	41.	20.	49.	25.	52.	30.	52.	35.	50.
	40.	48.												
351	5.	4.	10.	19.	15.	35.	20.	43.	25.	48.	30.	50.	35.	49.
	40.	48.	45.	46.										
352	5.	5.	10.	18.	15.	33.	20.	42.	25.	47.	30.	49.	35.	49.
	40.	47.	45.	44.										
353	5.	0.	10.	2.	15.	8.	20.	14.	25.	20.	30.	23.	35.	28.
	40.	32.	45.	35.	50.	36.	55.	36.	60.	37.	65.	37.	70.	38.
	75.	38.	80.	36.										
354	8.	3.	15.	12.	23.	28.	30.	43.	38.	56.	45.	65.	53.	70.
	60.	74.	68.	75.	75.	76.	83.	76.	90.	76.	98.	75.		
355	15.	5.	30.	22.	45.	33.	60.	37.	75.	39.	90.	38.		

LISTING OF RAW DATA OF TIME VRS CHART READING/

RUN NO	TIME	ER	TIME	ER	TIME	ER	TIME	ER	TIME	ER	TIME	ER	TIME	ER
356	5.	12.	10.	20.	15.	27.	20.	33.	25.	36.	30.	37.	35.	38.
	40.	39.	45.	40.	50.	40.								
357	5.	6.	10.	23.	15.	41.	20.	55.	25.	65.	30.	73.	35.	78.
	40.	81.	45.	83.	50.	82.	55.	80.	60.	79.				
358	5.	0.	10.	5.	15.	12.	20.	20.	25.	26.	30.	30.	35.	33.
	40.	35.	45.	37.	50.	38.	55.	38.	60.	38.	65.	38.	70.	37.
	75.	35.												
359	5.	0.	10.	0.	15.	9.	20.	15.	25.	20.	30.	25.	35.	29.
	40.	32.	45.	36.	50.	37.	55.	37.	60.	38.	65.	38.	70.	39.
	75.	39.	80.	38.	85.	37.	90.	37.						
360	15.	5.	30.	18.	45.	28.	60.	35.	75.	37.	90.	38.	105.	36.
361	15.	2.	30.	14.	45.	31.	60.	48.	75.	58.	90.	65.	105.	69.
	120.	70.	135.	70.	150.	70.								
362	15.	6.	30.	31.	45.	47.	60.	53.	75.	54.	90.	52.		
363	15.	2.	30.	8.	45.	28.	60.	43.	75.	55.	90.	65.	105.	68.
	120.	71.	135.	72.	150.	74.	165.	72.	180.	71.				

65

LISTING OF RAW DATA OF TIME VRS CHART READING/

RUN NO	TIME	ER	TIME	ER	TIME	ER	TIME	ER	TIME	ER	TIME	ER	TIME	ER
364	15.	2.	30.	13.	45.	31.	60.	48.	75.	61.	90.	36.	105.	72.
	120.	75.	135.	76.	150.	74.								
365	10.	2.	20.	16.	30.	35.	40.	46.	50.	52.	60.	54.	70.	53.
	80.	53.												
366	15.	3.	30.	12.	45.	33.	60.	50.	75.	60.	90.	67.	105.	68.
367	15.	7.	30.	31.	45.	54.	60.	70.	75.	77.	90.	79.	105.	78.
	120.	77.												
368	15.	12.	30.	42.	45.	64.	60.	77.	75.	81.	90.	83.		
369	5.	0.	10.	12.	15.	29.	20.	45.	25.	61.	30.	74.	35.	80.
	40.	85.	45.	88.	50.	90.	55.	92.	60.	91.	65.	91.	70.	89.
	75.	89.												
370	15.	1.	30.	1.	45.	10.	60.	21.	75.	32.	90.	41.	105.	47.
	120.	52.	135.	55.	150.	55.	165.	55.	180.	55.				
371	5.	0.	10.	20.	15.	43.	20.	61.	25.	77.	30.	86.	35.	91.
	40.	94.	45.	96.	50.	95.								
	5.	2.	10.	12.	15.	23.	50.	33.	25.	39.	30.	43.	35.	46.
	40.	46.	45.	46.	50.	47.								

LISTING OF RAW DATA OF TIME VRS CHART READING/

RUN NO	TIME	ER	TIME	ER	TIME	ER	TIME	ER	TIME	ER	TIME	ER	TIME	ER
372	15.	3.	30.	11.	45.	24.	60.	36.	75.	45.	90.	49.	105.	51.
	120.	52.	135.	52.	150.	52.								
373	5.	1.	10.	12.	15.	24.	20.	34.	25.	40.	30.	43.	35.	45.
	40.	46.	45.	47.	50.	46.	55.	45.	60.	43.	65.	42.		
374	5.	1.	10.	12.	15.	23.	20.	33.	25.	39.	30.	42.	35.	43.
	40.	44.	45.	45.	50.	45.								
375	15.	0.	30.	3.	45.	12.	60.	26.	75.	37.	90.	45.	105.	49.
	120.	51.	135.	53.	150.	52.								
376	5.	3.	10.	16.	15.	30.	20.	39.	25.	45.	30.	48.	35.	49.
	40.	48.	45.	48.	50.	47.								
377	5.	4.	10.	20.	15.	30.	20.	43.	25.	47.	30.	48.	35.	48.
	40.	47.	45.	45.										
378	15.	2.	30.	4.	45.	15.	60.	28.	75.	39.	90.	47.	105.	51.
	120.	52.	135.	52.	150.	53.	165.	52.						
379	5.	6.	10.	21.	15.	36.	20.	43.	25.	45.	30.	46.	35.	45.

LISTING OF RAW DATA OF TIME VRS CHART READING/

RUN NO	TIME	ER	TIME	ER	TIME	ER	TIME	ER	TIME	ER	TIME	ER	TIME	ER
380	15.	2.	30.	7.	45.	20.	60.	34.	75.	44.	90.	53.	105.	57.
	120.	58.	135.	59.										
381	15.	0.	30.	14.	45.	33.	60.	43.	75.	48.	90.	50.	105.	50.
382	15.	3.	30.	20.	45.	36.	60.	47.	75.	51.	90.	51.	105.	47.
383	15.	3.	30.	20.	45.	39.	60.	47.	75.	50.	90.	51.		
384	15.	4.	30.	25.	45.	43.	60.	51.	75.	52.	90.	51.		
385	15.	4.	30.	26.	45.	44.	60.	50.	75.	51.	90.	49.		
386	15.	6.	30.	29.	45.	45.	60.	51.	75.	-0.				
387	5.	0.	10.	3.	15.	7.	20.	14.	25.	20.	30.	27.	35.	30.
	5.	0.	10.	3.	15.	7.	20.	14.	25.	20.	30.	27.	35.	30.
	40.	33.	45.	35.	50.	37.	55.	39.	60.	39.	65.	41.	70.	40.
	75.	40.	80.	39.	85.	38.								
388	5.	2.	10.	17.	15.	31.	20.	39.	25.	44.	30.	45.	35.	45.
	40.	44.	45.	43.	50.	40.	55.	38.	60.	37.	65.	34.	70.	32.
	75.	31.	80.	30.	85.	28.								

LISTING OF RAW DATA OF TIME VRS CHART READING/

RUN NO	TIME	ER	TIME	ER	TIME	ER	TIME	ER	TIME	ER	TIME	ER	TIME	ER
389	15.	1.	30.	2.	6C.	16.	90.	35.	105.	44.	135.	60.	150.	65.
	180.	72.	210.	76.	270.	80.	300.	80.						
390	30.	3.	60.	16.	9C.	35.	120.	50.	150.	62.	180.	70.	210.	75.
	240.	78.	270.	80.	300.	79.								
391	30.	7.	60.	31.	90.	55.	120.	74.	150.	86.	180.	94.	210.	95.
	240.	93.	270.	92.										
392	30.	2.	60.	13.	90.	26.	120.	37.	150.	42.	180.	46.	210.	49.
	240.	48.												
393	30.	3.	60.	16.	90.	30.	120.	39.	150.	47.	180.	49.	210.	51.
394	30.	2.	60.	15.	90.	30.	120.	41.	150.	47.	180.	51.		
395	30.	4.	60.	23.	90.	38.	120.	47.	150.	50.	180.	51.	210.	50.
396	30.	4.	60.	25.	90.	42.	120.	49.	150.	53.	180.	53.	210.	50.
397	30.	6.	60.	27.	90.	44.	120.	51.	150.	53.	180.	52.	210.	48.
398	30.	9.	60.	33.	90.	45.	120.	51.	150.	51.	180.	49.	210.	47.
	240.	44.												

LISTING OF RAW DATA OF TIME VRS CHART READING/

RUN NO	TIME	ER	TIME	ER	TIME	ER	TIME	ER	TIME	ER	TIME	ER	TIME	ER
399	15.	2.	30.	15.	45.	30.	60.	40.	75.	47.	90.	51.	105.	51.
	120.	50.												
400	15.	5.	30.	21.	45.	39.	60.	48.	75.	52.	90.	52.	120.	51.
401	15.	5.	30.	24.	45.	40.	60.	47.	75.	52.	90.	51.	120.	51.
402	2.	6.	3.	35.	4.	56.	5.	68.	7.	77.	10.	79.	12.	77.
	15.	73.	17.	71.	20.	68.	22.	66.	25.	63.	27.	61.	30.	58.
	35.	52.	40.	48.	45.	44.	50.	41.						
403	10.	0.	20.	0.	20.	0.	40.	3.	50.	9.	60.	17.	70.	25.
	80.	31.	90.	36.	100.	39.	110.	42.	120.	44.	130.	46.	140.	47.
	150.	48.	180.	49.	210.	47.								
404	2.	4.	5.	60.	10.	75.	15.	71.	20.	68.	25.	63.	30.	57.
	35.	52.	40.	48.	45.	45.	50.	42.						
405	10.	0.	20.	0.	30.	0.	40.	4.	50.	10.	60.	18.	70.	25.
	80.	32.	90.	37.	100.	40.	110.	42.	120.	44.	130.	46.	140.	47.
	150.	47.	160.	48.	170.	48.	180.	49.						
406	15.	0.	30.	0.	45.	6.	60.	17.	75.	27.	90.	38.	105.	45.
	120.	51.	135.	56.	150.	60.	165.	59.	180.	60.				

LISTING OF RAW DATA OF TIME VRS CHART READING/

RUN NO	TIME	ER	TIME	ER	TIME	ER	TIME	ER	TIME	ER	TIME	ER	TIME	ER
407	5.	6.	10.	36.	15.	65.	25.	68.	30.	70.	35.	71.	40.	71.
	45.	69.	50.	68.	60.	64.	70.	60.	80.	57.				
408	5.	5.	10.	41.	15.	55.	20.	60.	25.	63.	30.	65.	35.	67.
	40.	68.	45.	67.	50.	66.	60.	62.	70.	58.	80.	55.	90.	51.
	100.	48.												
409	5.	8.	10.	32.	15.	50.	20.	60.	25.	64.	30.	67.	35.	68.
	40.	68.	45.	67.	50.	65.	55.	63.	60.	61.	70.	58.	80.	54.
	90.	50.												
410	5.	7.	10.	21.	15.	28.	20.	33.	25.	37.	30.	37.	35.	34.
	40.	35.	45.	34.	50.	33.	60.	31.	70.	28.	80.	25.		
411	5.	8.	10.	21.	15.	29.	20.	32.	25.	33.	30.	34.	35.	34.
	40.	33.	45.	32.	50.	30.	50.	28.	60.	28.	70.	25.	80.	22.
	90.	20.												
412	5.	6.	10.	18.	15.	26.	20.	31.	25.	32.	30.	32.	35.	32.
	40.	30.	45.	28.	50.	27.	55.	26.	60.	24.	70.	21.	80.	18.
	90.	17.												
413	5.	12.	10.	38.	15.	53.	20.	59.	25.	62.	30.	61.	35.	58.
	40.	55.	45.	51.	50.	49.	55.	45.	60.	43.	70.	38.	80.	35.

LISTING OF RAW DATA OF TIME VRS CHART READING/

RUN NO	TIME	ER	TIME	ER	TIME	ER	TIME	ER	TIME	ER	TIME	ER	TIME	ER
414	5.	10.	10.	40.	15.	53.	20.	59.	25.	60.	30.	59.	35.	56.
	90.	29.												
415	30.	1.	60.	8.	90.	16.	120.	23.	150.	26.	180.	28.	210.	29.
	240.	28.	270.	28.	300.	28.	360.	27.	420.	26.	480.	23.		
416	5.	17.	10.	42.	15.	56.	20.	61.	25.	61.	30.	57.	35.	59.
	40.	50.	50.	41.	60.	36.	75.	30.						
417	30.	0.	60.	11.	90.	24.	120.	33.	150.	37.	180.	36.	210.	32.
	240.	27.	270.	23.										
418	60.	0.	120.	6.	180.	19.	240.	31.	300.	38.	360.	43.	420.	46.
	480.	45.												
419	60.	2.	120.	9.	180.	22.	240.	31.	300.	38.	360.	41.	420.	43.
420	60.	0.	120.	4.	180.	18.	240.	29.	300.	34.	360.	36.	400.	37.
421	60.	0.	120.	9.	180.	21.	240.	30.	300.	33.	360.	35.	400.	35.
	420.	34.												
422	60.	0.	120.	10.	180.	22.	240.	30.	300.	33.	360.	34.		

LISTING OF RAW DATA OF TIME VRS CHART READING/

RUN NO	TIME	ER	TIME	ER	TIME	ER	TIME	ER	TIME	ER	TIME	ER	TIME	ER
423	60.	0.	120.	11.	180.	24.	240.	30.	300.	33.	360.	33.		
424	60.	0.	120.	10.	180.	23.	240.	30.	300.	34.	360.	35.	420.	34.

END-OF-DATA ENCOUNTERED ON SYSTEM INPUT FILE.

REFERENCES

1. Woodward, D. H.: J. Opt. Soc. Am. vol. 54, 1964, p. 1325.

2. Chandrasekhar, S.: Radiative Transfer. New York, Dover Publications, Inc., 1960.

3. Chu, C. M., Churchill, S. W., and Pang, S. C.: Electromagnetic Scattering. New York, Pergamon Press, 1963, p. 507.

4. Wolley, R. and Stibbs, D. W. N.: The Outer Layers of a Star. London, Clarendon Press, 1953.

5. Munch, G.: Stellar Atmospheres. Ed. J. J. Greenstein. Chicago, University of Chicago Press, 1960, pp. 1-49.

6. Murry, B. C. and Wildey, R. L.: Astrophys. J. vol. 137, 1963, p. 692.

7. Hamaker, H. C.: Philips Research Repts. vol. 2, 1947, p. 55.

8. Eckert, E. R. G., Sparrow, E. M., Ibele, W. E., and Goldstein, R. J.: Internat. J. Heat Mass Transfer (G. B.), vol. 6, 1963, p. 971.

9. Aberdeen, J. and Laby, T. H.: Proc. Roy. Soc. (London). vol. A113, 1926, p. 459.

10. Kannuluik, W. G., Knight, F., and Martin, L. H.: Proc. Roy. Soc. (London). vol. A141, 1933, p. 144.

11. Rayleigh, L.: Phil. Mag. vol. 34, 1892, p. 481.

12. Burgers, H. C.: Physik. Z. vol. 20, 1919, p. 73.

13. Russell, H. W.: J. Am. Ceram. Soc. vol. 18, 1935, p. 1.

14. Wechsler, A. E. and Glaser, P. E.: ICARUS. vol. 4, 1965, p. 335.

15. Wesselink, A. J.: Astron. Inst. of Netherlands. vol. 10, 1948, p. 351.

16. Laubitz, M. J.: Can. J. Phys. vol. 37, 1959, p. 798.

REFERENCES (Continued)

17. Schotte, W.: Am. Inst. Chem. Engrs. J. vol. 6, 1960, p. 63.

18. Dekker, A. J.: Solid State Physics. New Jersey, Prentice-Hall, Inc., 1957, p. 296.

19. Moore, C. J.: Heat Transfer Across Surfaces in Contact. Southern Methodist University Institute of Technology Report, 67-2, March 1967.

20. Halajian, J. D., Reichman, J., and Karafiath, L. L.: Correlation of Mechanical and Thermal Properties of Extraterrestrial Materials. Grumman Research Department Report RE-280, January 1967, p. 17.

21. Watson, K.: The Thermal Conductivity Measurements of Selected Silicate Powders in Vacuum From 150° - 350° K. Thesis, The California Institute of Technology, Pasadena, California, 1964. p. 200.

22. Bernett, E. C., Wood, H. L., Jaffe, L. D., and Marlens, H. E.: AIAA, vol. 1, 1963, p. 1402.

23. Bernett, E. C., Wood, H. L., Jaffe, L. D., and Marlens, H. E.: Thermal Properties of a Simulated Lunar Material in Air and in Vacuum. Jet Propulsion Laboratory, Technical Report 32-368, November 25, 1962.

24. Everest, A., Glaser, P. E., and Wechsler, A.: Thermal Conductivity of Non-Metallic Materials. Arthur D. Little Co. Report, April 1962.

25. Blackwell, J. H.: J. of Appl. Phys. vol. 25, 1954, p. 137.

26. Jaeger, J. C.: Australian J. Phys. vol. 12, 1959, p. 203.

27. Blackwell, J. H.: Can. J. Phys. vol. 34, 1956, p. 412.

28. Jaeger, J. C. and Sass, J. H.: Brit. J. Appl. Phys. vol. 15, 1964, p. 1187.

REFERENCES (Concluded)

29. Wechsler, A. E. and Simon, I.: Thermal Conductivity and Dielectric Constant of Silicate Materials. Arthur D. Little Co. Report, December 1966.

30. Carslaw, H. S. and Jaeger, J. C.: Conduction of Heat in Solids. Second edition, London, Oxford Press, 1959, pp. 354-356.

31. Mathews, F. and Walker, R. L.: Mathematical Methods of Physics. New York, W. A. Benjamin, Inc., 1964, p. 231.

32. Carslaw, H. S. and Jaeger, J. C.: Conduction of Heat in Solids. Second edition, London, Oxford Press, 1959, p. 261.

33. Davidon, William C.: Variable Metric Method for Minimization. Argonne National Laboratory, Lemont, Illinois, 1959.

34. Kittel, C.: Introduction to Solid State Physics. Second edition, New York, John Wiley and Sons, Inc., 1959, p. 139.

35. Goldsmith, A., Waterman, T. E., and Huschhorn, H. J.: Handbook of Thermophysical Properties of Solid Materials. vol. 3, New York, Pergamon Press, 1961, p. 769.

36. Watson, K.: The Thermal Conductivity Measurements of Selected Silicate Powders in Vacuum from 150° - 350° K. Thesis, The California Institute of Technology, Pasadena, California, 1964, p. 11.

"The aeronautical and space activities of the United States shall be conducted so as to contribute . . . to the expansion of human knowledge of phenomena in the atmosphere and space. The Administration shall provide for the widest practicable and appropriate dissemination of information concerning its activities and the results thereof."

— NATIONAL AERONAUTICS AND SPACE ACT OF 1958

NASA SCIENTIFIC AND TECHNICAL PUBLICATIONS

TECHNICAL REPORTS: Scientific and technical information considered important, complete, and a lasting contribution to existing knowledge.

TECHNICAL NOTES: Information less broad in scope but nevertheless of importance as a contribution to existing knowledge.

TECHNICAL MEMORANDUMS: Information receiving limited distribution because of preliminary data, security classification, or other reasons.

CONTRACTOR REPORTS: Scientific and technical information generated under a NASA contract or grant and considered an important contribution to existing knowledge.

TECHNICAL TRANSLATIONS: Information published in a foreign language considered to merit NASA distribution in English.

SPECIAL PUBLICATIONS: Information derived from or of value to NASA activities. Publications include conference proceedings, monographs, data compilations, handbooks, sourcebooks, and special bibliographies.

TECHNOLOGY UTILIZATION PUBLICATIONS: Information on technology used by NASA that may be of particular interest in commercial and other non-aerospace applications. Publications include Tech Briefs, Technology Utilization Reports and Notes, and Technology Surveys.

Details on the availability of these publications may be obtained from:

SCIENTIFIC AND TECHNICAL INFORMATION DIVISION

NATIONAL AERONAUTICS AND SPACE ADMINISTRATION
Washington, D.C. 20546